

# Proper motions of young stars in Chamaeleon

## I. A Virtual Observatory study of spectroscopically confirmed members

Belén López Martí<sup>1</sup>, Francisco Jiménez-Esteban<sup>1,2,3</sup>, Amelia Bayo<sup>4</sup>, David Barrado<sup>1,5</sup>, Enrique Solano<sup>1,2</sup>, and Carlos Rodrigo<sup>1,2</sup>

<sup>1</sup> Centro de Astrobiología (INTA-CSIC), Departamento de Astrofísica, P.O. Box 78, E-28261 Villanueva de la Cañada, Madrid, Spain  
e-mail: belen@cab.inta-csic.es

<sup>2</sup> Spanish Virtual Observatory, Spain

<sup>3</sup> Saint Louis University, Madrid Campus, Division of Science and Engineering, Avenida del Valle 34, E-28003 Madrid, Spain

<sup>4</sup> European Southern Observatory, Alonso de Córdova 3107, Vitacura, Santiago, Chile

<sup>5</sup> Calar Alto Observatory, Centro Astronómico Hispano-Alemán, C/ Jesús Durbán Remón 2-2, E-04004 Almería, Spain

Received; accepted

### ABSTRACT

**Context.** The study of the motion of the members of a given open cluster or stellar association provides key information about their formation and early evolution. The Chamaeleon cloud complex constitutes one of the closest and best studied low-mass star-forming regions in the Galaxy.

**Aims.** We want to provide further evidence of the origin of the proposed stellar members of Chamaeleon and to identify interlopers from the foreground  $\epsilon$  Cha and  $\eta$  Cha associations.

**Methods.** We compile lists of spectroscopically confirmed members of Chamaeleon I and II,  $\epsilon$  Cha and  $\eta$  Cha, and of background objects in the same line of sight. Using Virtual Observatory tools, we cross-match these lists with the UCAC3 catalogue to get the proper motions of the objects. In the vector point diagram, we identify the different moving groups, and use this information to study the membership of proposed candidate members of the associations from the literature. For those objects with available radial velocities, we compute their Galactic space velocities. We look for correlations between the known properties of the objects and their proper motions.

**Results.** The members of the dark clouds exhibit clearly different proper motions from those of the foreground associations and of the background stars. The data suggest that Chamaeleon II could have different dynamical properties from Chamaeleon I. Although the two foreground clusters  $\epsilon$  and  $\eta$  Chamaeleontis constitute two different proper motion groups, they have similar spatial motions, which are different from the spatial motion of Chamaeleon I. On the other hand, the space motions of the Chamaeleon II stars look more similar to those of the foreground clusters than to the Chamaeleon I stars, but the numbers are low. We find no correlations between the proper motions and the properties of the objects in either of the clouds.

**Conclusions.** On the basis of proper motion, Chamaeleon I and II constitute two physical entities unrelated to the foreground  $\epsilon$  and  $\eta$  Chamaeleontis clusters, but with the available data it is unclear to what extent the stellar populations in both clouds are physically connected to each other.

**Key words.** stars:low-mass, brown dwarfs – stars: kinematics and dynamics – stars: formation – stars: luminosity function, mass function – astronomical databases: miscellaneous – astronomical databases: virtual observatory tools

## 1. Introduction

The kinematic properties of the members of a given stellar association hold important clues to its history. Some formation models predict that the early dynamical evolution of the parent proto-stellar cluster should lead to mass-dependent kinematic distributions, and, eventually, to an efficient mass segregation (Kroupa & Bouvier 2003), while other numerical simulations predict similar kinematic properties over the whole mass spectrum (Bate 2012). Various authors have used radial velocity measurements to study the kinematic properties of young low-mass objects (e.g. Jeffries et al. 2006; Maxted et al. 2008), and a number of surveys have used proper motions to identify and confirm new low-mass members in young associations and clusters (e.g. Moraux et al. 2001; Kraus & Hillenbrand 2007; Bouy & Martín 2009; Caballero 2010). In particular, our recent proper motion study of the Lupus star-forming region shows that it is possible to distinguish between probable low-mass members of the complex

and likely contaminants using kinematic information from available astrometric catalogues (López Martí et al. 2011, hereafter LJS11).

The Chamaeleon complex is one of the closest and best studied low-mass star-forming regions. At an estimated distance in the range 115-215 pc, it is composed of three dark clouds, named Chamaeleon I, II and III (Schwartz 1977; Schwartz et al. 1991). The oldest one is Chamaeleon I, with a mean age of about 2 Myr; it contains more than 300 known young stars (see Luhman 2008, for the latest census), most of them clustered in two cloud cores containing two intermediate-mass stars, HD 97048 and HD 97300. Chamaeleon II seems to be at an earlier stage of evolution than Chamaeleon I, because it contains more embedded than visual objects (Gauvin & Strom 1992). Surveys by several authors have identified more than 60 stars in this cloud (Spezzi et al. 2007, 2008; Alcalá et al. 2008, and references therein). No active star formation seems to be taking place in Chamaeleon III.

The Chamaeleon clouds have also been the target of kinematic studies, generally based on radial velocities and focused on the brightest stars in the complex (e.g. Dubath et al. 1996). The exceptions are a few very low-mass stars and brown dwarf candidates in Chamaeleon I (Joergens 2006, and references therein). Proper motion and parallax information from Hipparcos has been used to assess the origin of the star formation in the clouds and their relation to other neighbouring associations (Sartori et al. 2003). X-ray observations during the past two decades, combined with Hipparcos astrometry, have shown that the young stars observed towards the Chamaeleon sky area can be grouped into several distinct associations: the Chamaeleon dark cloud complex itself, and the foreground (at around 100 pc)  $\epsilon$  Chamaeleontis ( $\epsilon$  Cha) and  $\eta$  Chamaeleontis ( $\eta$  Cha) young associations (Feigelson et al. 2003; Mamajek et al. 1999). The observations have shown that these two associations are older than the Chamaeleon star-forming complex ( $\sim 15$ -20 Myr), but it is unclear whether there is a relation between the two, or whether they are somehow related to the dark clouds.

In this paper, we make use of proper motions from the Third US Naval Observatory CCD Astrograph Catalog (UCAC3; Zacharias et al. 2010) and of Virtual Observatory<sup>1</sup> (VO) tools to investigate the kinematic properties of members and candidate members of the Chamaeleon dark clouds. Our goals are to provide further evidence of a common origin for all these objects and to test their association with the dark clouds and between the clouds themselves.

## 2. Available data

### 2.1. Object compilation

We compiled a list of Chamaeleon confirmed members (through spectroscopy) from the literature. For Chamaeleon I, we retrieved the list from the most recent census by Luhman (2007), and completed it with the eight new members reported by Luhman & Muench (2008a). The final list contained 304 objects down to  $R = 24$  mag, with extinctions in the range  $A_V \approx 0$ -20 mag). For Chamaeleon II, we used the list of confirmed members from Spezzi et al. (2008), which includes all objects studied in previous works. In total, we had 41 Chamaeleon II spectroscopically confirmed members, with  $R$ -band magnitudes down to about 23 mag and extinctions in the range  $A_V \approx 0$ -11 mag.

To assess how clearly we can separate the different populations based on the available proper motions, and to check the possible presence of interlopers from the foreground clusters in our Chamaeleon I and II lists, we compiled two lists of members for the  $\epsilon$  Cha and  $\eta$  Cha associations, merging the catalogues provided by Luhman (2004) and Fernández et al. (2008) for both groups, and adding the objects from the lists by Luhman & Steeghs (2004) in  $\eta$  Cha and by da Silva et al. (2009) in  $\epsilon$  Cha. Membership of these objects in the corresponding cluster has been confirmed by several different means, including spectroscopy and proper motions. The final compiled lists contained 36 stars in  $\epsilon$  Cha and 20 in  $\eta$  Cha down to  $R \sim 18$  mag. No estimations of extinction are available for these stars, but their location outside areas of dense dust suggests that it is very low in most cases.

For control purposes, we also considered the list of 88 background sources from Table 4 of Luhman (2007). These objects

were initially proposed in the literature as Chamaeleon I members, but they were later discarded through spectroscopy.

We note that the magnitude limit of most of these compilations is much fainter than the UCAC3 magnitude limit (see Sect. 2.2 below); therefore, a significant fraction of objects are not expected to have counterparts in that catalogue. Since the faintest objects are also the lowest mass ones, and given that the substellar mass limit is estimated to be around  $R \sim 21$  mag at the age and distance of the Chamaeleon clouds, this implies that only stellar members of the associations will have measured proper motions. In particular, the objects at the substellar boundary studied by López Martí et al. (2004) in Chamaeleon I and Barrado y Navascués & Jayawardhana (2004) in Chamaeleon II are not included in UCAC3.

In a second step in our study, we also investigated those candidate members of the Chamaeleon associations from the literature whose true nature is still unclear. This list included 63 X-ray emitting stars unveiled by the ROSAT mission (Alcalá et al. 1995) that remained unclassified, as well as some objects from other previous works still lacking spectroscopic confirmation of youth: the list of uncertain objects provided by Luhman et al. (2004, his Table 8; 21 objects) for Chamaeleon I, and the candidate members of Chamaeleon II without spectroscopic confirmation of membership from Spezzi et al. (2008, 11 objects) and the DENIS survey (Vuong et al. 2001, 41 objects).

In total, our list of unconfirmed candidates amounted to 136 objects (63 ROSAT stars and 73 objects from other works), but the vast majority of them are too faint to be included in the proper motion study, and only a handful of them have proper motion measurements available in UCAC3, as explained in Sect. 4.

### 2.2. Proper motion data

To get proper motion measurements, we cross-matched our compiled catalogues with the UCAC3 catalogue, available within the Virtual Observatory. This is an all-sky survey containing about 100 million objects, 95% of them with proper motions, covering a dynamical range of about 8-16 mag in a single bandpass between V and R. Its positional accuracy is about 15 to 100 mas per coordinate, depending on magnitude. The proper motion errors range from 1 to 10 mas/yr, depending on magnitude and observing history.

As in our previous work on Lupus (LJS11), we followed a VO-based methodology to cross-match and analyse the data. We made use of the Multiple Cone Search utility of TOPCAT<sup>2</sup>. A matching radius of  $2''$  was used. We retained all sources whose proper motion errors were not set to zero, which had been computed using more than two epoch positions, and which had an object classification flag (ot) between 0 and 3. After purging the data in this way, the number of counterparts with proper motion data in Chamaeleon I and II were 81 and 25 (corresponding to the 27% and 61% of the total number of stars included in our compiled lists), respectively. In addition, UCAC3 provided proper motions for 19 objects in  $\epsilon$  Cha and 12 in  $\eta$  Cha, respectively (53% and 60% of the compiled lists, respectively). As for the background sources, the number of objects with available proper motions was 52 (59%). These samples were further cleaned by removing bad proper motion measurements and interlopers identified during the analysis (see Sect. 3 for details). The proper motion data for the members of the dark clouds,

<sup>1</sup> The VO is a project designed to provide the astronomical community with the data access and the research tools needed to enable the exploration of the digital, multiwavelength universe resident in the astronomical data archives. <http://www.ivoa.net>

<sup>2</sup> TOPCAT is an interactive graphical viewer and editor for tabular data that allows the user to examine, analyse, combine, and edit astronomical tables. <http://www.star.bris.ac.uk/~mbt/topcat/>

the foreground clusters, and the contaminants are presented in Tables 1, 2, and 3, respectively.

In LJS11, a comparison of the cross-matching results of the Lupus catalogues with different astrometric catalogues (USNO-B1, SuperCOSMOS, PPMX) led to the conclusion that UCAC3 provided the best compromise between the number of counterparts (dependent among others on the magnitude limit of the catalogue) and the typical proper motion errors. For the present work, we further compared the analysis presented in Sect. 3.1 with the results obtained using the recently released PPMXL catalogue (Röser et al. 2010). Although this catalogue is deeper in magnitude than UCAC3, and thus included much more sources from our initial member lists, it was not possible to distinguish the different populations due to the larger errors in the proper motions for most of the objects. Thus, we concluded that UCAC3 is still the best option available for our study.

### 2.3. Complementary data

#### 2.3.1. Radial velocities

Aiming at better insight into the kinematics of the members of the Chamaeleon associations, we combined the UCAC3 proper motions with radial velocity measurements from the literature (Covino et al. 1997; Joergens & Guenther 2001; Biazzo et al. 2012) and from the SIMBAD database. We only considered measurements with errors better than about 30%. If several measurements were available for the same star, the average was computed. Known and suspected spectroscopic binaries were discarded.

Our final sample contains radial velocity information for 18 stars in Chamaeleon I and nine in Chamaeleon II. These data are summarized in Table 1. We also retrieved radial velocity data for 15 stars in the  $\epsilon$  Cha association and four stars in the  $\eta$  Cha association, which are listed in Table 2. We also considered radial velocities from Covino et al. (1997) for the candidate members of the associations discussed in Sect. 4.1.

#### 2.3.2. Photometry

We compiled multiwavelength photometry for the confirmed members and candidate members of the Chamaeleon associations discussed in this work. Most of the data were retrieved using the latest version of the VO SED Analyzer tool<sup>3</sup> (VOSA; Bayo et al. 2008, submitted). They include ultraviolet photometry from GALEX (Bianchi & GALEX Team 2000), optical photometry ( $B$ ,  $V$  and  $I$ ) from the Tycho-2 and DENIS catalogues (Høg et al. 2000; DENIS Consortium 2005), near-infrared photometry from 2MASS (Skrutskie et al. 2006), and mid-infrared photometry from AKARI and WISE (Ishihara et al. 2010; Cutri & et al. 2012).

More photometry data from the literature were retrieved through the VizieR catalogue service (Ochsenbein et al. 2000). For Chamaeleon II members and candidate members, we retrieved the compilation of optical and infrared photometry by Alcalá et al. (2008), which includes Johnson  $U$ -band data from Hughes & Hartigan (1992), Cousins  $R_C I_C$  and Sloan  $z$  photometry from Spezzi et al. (2007), and mid- and far-infrared photometry from IRAS and from the “cores to disks” ( $c2d$ ) *Spitzer* legacy programme (Evans et al. 2003).<sup>4</sup> For Chamaeleon I members and

candidate members, we retrieved the *Spitzer*/IRAC and MIPS 24  $\mu$ m photometry provided by Luhman & Muench (2008a). Optical photometry from the survey by López Martí et al. (2004) was also included in the data compilation for this cloud, as well as IRAS fluxes for three objects. The photometric information is summarized in Table 4.<sup>5</sup>

## 3. Kinematic groups towards Chamaeleon

### 3.1. Identification of proper motion groups

Figure 1 shows the vector point diagram for the young sources seen towards the Chamaeleon sky area that are included in the UCAC3 astrometric catalogue. In Fig. 2 we can see the histograms of the total proper motion modulus for the Chamaeleon I and II members, for the members of the foreground associations, and for the known background contaminants. As expected, the young objects are clearly separated from the older background objects in these plots, and several distinct kinematic groups can be seen, which correspond to different spatial locations in the sky (see Fig. 3).

The spectroscopically confirmed members of Chamaeleon I (hereafter “the Cha I moving group”) are clustered in the same area of the vector-point diagram, roughly around the position  $(-19, +2)$  mas/yr. The Chamaeleon II objects, on the other hand, are seen mostly clustered around the position  $(-25, -7)$  mas/yr, slightly shifted from the Chamaeleon I sources (Fig. 1). This seems to suggest that these objects (hereafter “the Cha II moving group”) are moving, on average, faster than the Chamaeleon I stars in the tangential direction. This is also seen in the shift of the peak of the total proper motion distribution in Chamaeleon II with respect to Chamaeleon I (Fig. 2). If real, this result is interesting, because all estimations in the literature place Chamaeleon II at the same distance or further away than Chamaeleon I; hence, the difference in proper motion between both populations cannot be attributed to distance. However, the difference in mean proper motions is of little significance owing to the low number of Chamaeleon II sources with measured proper motions, and to the large dispersion.

The two foreground associations form in turn two distinct kinematic groups in the vector point diagram, which are clearly different from those in the dark clouds. The mean UCAC3 proper motions for these two groups are in good agreement with previously published values (Kharchenko et al. 2005; Wu et al. 2009). Interestingly, the total proper motion is very similar in both associations, as shown by the histograms in Fig. 2. As shown later in Sect. 3.3, the radial velocities of the stars in both clusters are also very similar.

Finally, with a few exceptions, the objects classified as background contaminants have lower proper motion values than any of the young moving groups and are clustered in a different location of the vector point diagram. This confirms our ability to distinguish members and non-members of the Chamaeleon associations with the UCAC3 data. Even so, the separation between the groups is not complete, and there is some overlapping between young stars and contaminants and between young stars from different groups.

A few spectroscopically confirmed members from both Chamaeleon clouds present UCAC3 proper motions that are clearly discrepant from those of their attributed associations. To check the reliability of the reported measurements, we followed the same procedure as in LJS11: Using *Aladin*, we visually inspected these objects, blinking and comparing two sets of images

<sup>3</sup> <http://svo2.cab.inta-csic.es/svo/theory/vosa/>

<sup>4</sup> The  $c2d$  data are now retrievable through VOSA (Bayo et al. submitted).

<sup>5</sup> Available online.

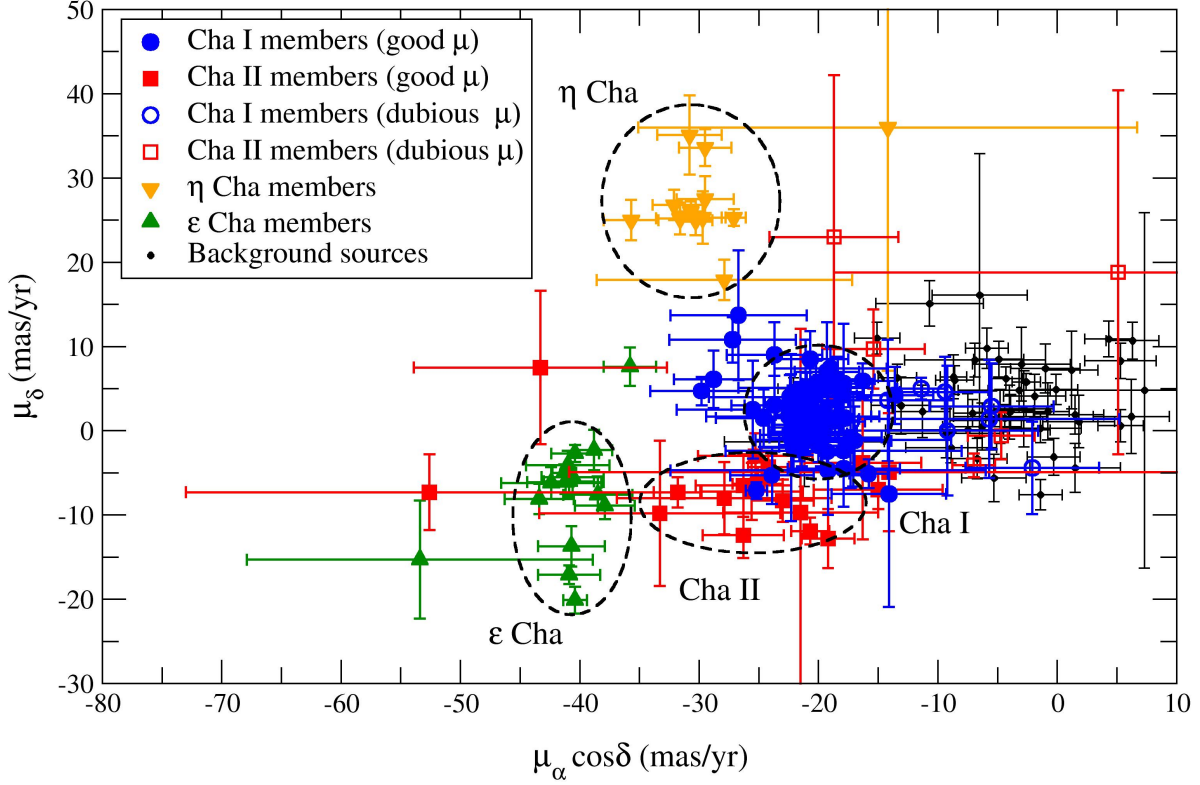


**Fig. 1.** UCAC3 vector point diagram for the objects seen towards the Chamaeleon sky area. Only spectroscopically confirmed members are considered. Sources belonging to different kinematic associations and to the background have been plotted with different symbols and colours. Objects with reliable and dubious proper motions have been indicated with solid and open symbols, respectively (see Sect. 3.1 for details). To help the eye, the moving groups have been labelled and marked with ellipses. Some interlopers (objects with discrepant proper motions that are more likely members of other associations) are identified (see discussion in Sect. 3.4).

separated several decades in time, from the optical POSS and the near-infrared 2MASS surveys (Skrutskie et al. 2006). The 2MASS sources and the UCAC3 counterparts were superimposed on the images to assess the reliability of the cross-match. Besides, we used other available astro-photometric databases, namely the Astrographic Catalogue AC2000.2 (Urban et al. 1998) and the SuperCOSMOS Sky Survey (Hambly et al. 2001) to verify the peculiar proper motions, and the USNO-B Catalog (Monet et al. 2003) and the PPMX and PPMXL catalogues (Röser et al. 2008, 2010) for comparison. This procedure showed that the clearly discrepant proper motions were mostly caused by errors in the measurements, mainly from centroiding errors or source confusion. A rough estimation of the proper motions of the objects, based on the comparison of the positions measured by the different catalogues, and with the motion of other nearby cloud members, suggests that most of them have proper motions in relatively good agreement with the corresponding moving groups.

The reliability of the proper motions is difficult to assess in some cases (e.g. HD 104237D and E) because these sources are part of visual binaries or multiples not always resolved in the images. And in a few cases (e.g. CW Cha), we could not test the proper motions in this way because SuperCOSMOS provides no data for the stars, or else the data were wrong. The sources with

clearly wrong proper motions (7 from Chamaeleon I and 2 from Chamaeleon II) were removed from the vector point diagram of Fig. 1. They were also excluded from Tables 1 and 2. Objects with dubious proper motions (because they could not be tested or the checks were inconclusive) were not removed from the tables, but a flag was added.

We also identified four spectroscopically confirmed members (2MASS J11183572-7935548, CM Cha, Sz 60W, and CP-68 1388) whose UCAC3 proper motions seem to be right but do not agree with the means of their attributed associations; these interlopers are discussed in Sect. 3.4 below.

### 3.2. Stars with Hipparcos and Tycho measurements

Five Chamaeleon I and three  $\epsilon$  Cha bona fide members from our UCAC3 samples have proper motion and parallax measurements provided by the latest Hipparcos reduction (van Leeuwen 2007). In addition, six  $\epsilon$  Cha and two  $\eta$  Cha members have proper motions from the Tycho catalogue (Høg et al. 1998). These data are summarized in Table 5, together with the parallax, if available, and the distance derived from it. We used this information as a further check of the accuracy of the UCAC3 measurements.

We note that the proper motions of bright stars in UCAC3 are based on about 140 catalogues, including Hipparcos and Tycho.

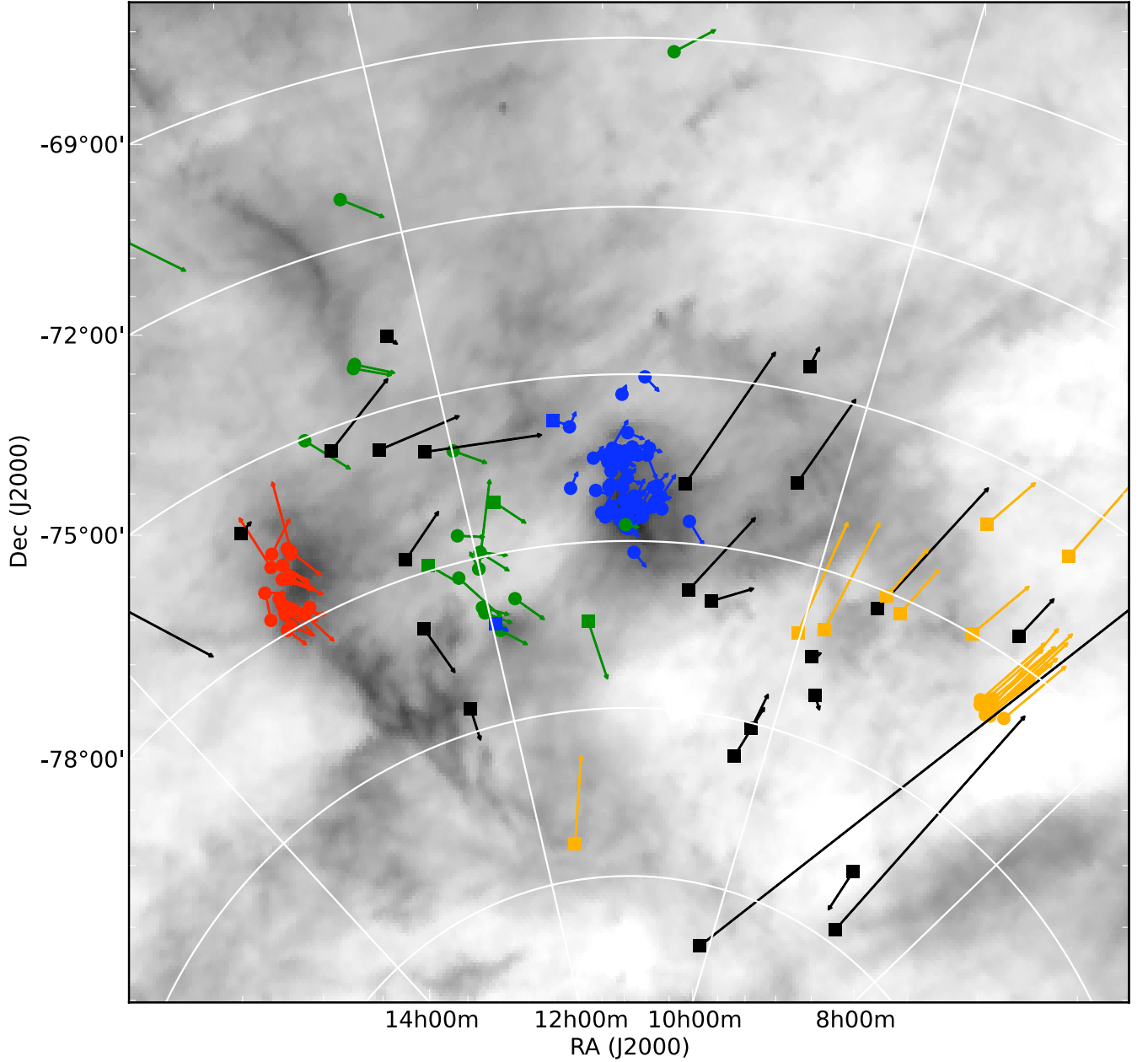


**Fig. 3.** Current spatial location of the members of the Chamaeleon associations (circles) and of the ROSAT sources discussed in Sect. 4.1 (squares). Colours as in Fig. 1. Also shown are the expected displacement of these objects within  $10^5$  Myr. The background image is a dust map by Schlegel et al. (Schlegel et al. 1998). Only objects with reliable proper motions are considered.

Therefore, we generally expect good agreement between the UCAC3 measurements and the proper motions listed in Table 5, as is indeed found. However, problems may have affected the measurements in some of the images used by UCAC3, either due to saturation, nebulosity, or the presence of nearby fainter stars. This seems to be the case for two Chamaeleon I stars (HD 97300 and CW Cha). For these two objects, the Hipparcos proper motions are in much better agreement with membership in the Cha I moving group than the UCAC3 values.

In particular, the membership in the dark cloud of HD 97300 (the intermediate-mass star seen towards the northern core of Chamaeleon I) and its evolutionary status have sometimes been questioned. However, most authors agree that this is most likely a Herbig Ae/Be star similar to HD 97048 in the southern

Chamaeleon I core. The proper motion seems to confirm that this star is a member of the Chamaeleon I cloud.

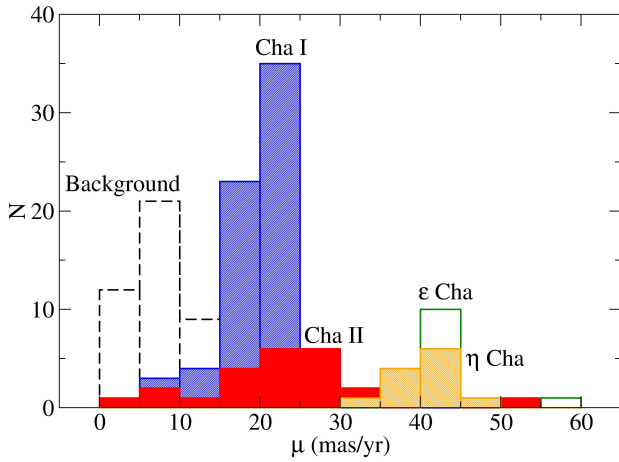
It is also interesting to note that HD 97048 has been included in the catalogue of potential young runaway stars by Tetzlaff et al. (2011), albeit with not very high probability (61%). However, we notice that the selection by these authors is only based on Hipparcos stars, which are relatively bright. Therefore, the sample used by Tetzlaff et al. (2011) included only a handful of Chamaeleon I members. Indeed, Table 5 shows that the proper motion of this object is lower, in modulus, than the rest of Chamaeleon I stars with Hipparcos or Tycho measurements, what could be interpreted as a hint for a different motion pattern. However, when the larger sample of cloud members provided by the UCAC3 catalogue are considered, HD 97048 does not stand up as having remarkably different kinematical properties from

**Table 5.** Hipparcos and Tycho proper motions and Hipparcos parallaxes for Chamaeleon stars

Name	UCAC3		Hipparcos/Tycho		$\pi$ (mas)	$d$ (pc)	Reference <sup>a</sup>	Remarks <sup>b</sup>
	$\mu_{\alpha} \cos \delta$ (mas/yr)	$\mu_{\delta}$ (mas/yr)	$\mu_{\alpha} \cos \delta$ (mas/yr)	$\mu_{\delta}$ (mas/yr)				
Chamaeleon I cloud								
HD 93828	$-25.2 \pm 0.9$	$-7.1 \pm 1.0$	$-26.72 \pm 0.99$	$-8.91 \pm 0.84$	$5.70 \pm 0.96$	$175 \pm 30$	H	
HD 97048	$-17.8 \pm 0.8$	$1.5 \pm 0.8$	$-18.64 \pm 0.72$	$+2.18 \pm 0.62$	$6.31 \pm 0.62$	$158 \pm 16$	H	
HD 97300	$-17.7 \pm 1.0$	$-2.7 \pm 1.1$	$-21.63 \pm 0.94$	$-0.72 \pm 0.78$	$5.60 \pm 0.88$	$178 \pm 28$	H	d
CV Cha	$-21.3 \pm 1.1$	$1.9 \pm 1.0$	$-20.82 \pm 2.95$	$+1.32 \pm 2.78$	$6.97 \pm 2.86$	$143 \pm 59$	H	
CW Cha	$-13.6 \pm 3.2$	$4.2 \pm 3.4$	$-26.05 \pm 3.82$	$-6.46 \pm 3.55$	$3.92 \pm 3.56$	$255 \pm 232$	H	d
$\epsilon$ Chamaeleontis cluster								
CP-68 1388	$-35.8 \pm 2.2$	$7.6 \pm 2.3$	$-36.3 \pm 1.9$	$+4.7 \pm 1.6$			T	
T Cha	$-41.2 \pm 3.2$	$-6. \pm 1.4$	$-33.45 \pm 3.87$	$-9.36 \pm 2.97$	$6.11 \pm 2.96^c$	$164 \pm 79$	H	d
DW Cha	$-40.4 \pm 2.0$	$-2. \pm 1.0$	$-41.7 \pm 1.62$	$+0.13 \pm 1.4$	$11.06 \pm 1.52$	$90 \pm 12$	H	
RX J1159.7-7601	$-40.9 \pm 2.1$	$-6. \pm 1.8$	$-40.53 \pm 1.66$	$-5.83 \pm 1.49$	$9.89 \pm 1.72$	$101 \pm 18$	H	
HD 104467	$-41.3 \pm 1.0$	$-5. \pm 1.0$	$-39.8 \pm 1.7$	$-6.3 \pm 1.6$			T	
HD 105923	$-37.9 \pm 2.5$	$-8. \pm 1.6$	$-37.6 \pm 1.7$	$-7.7 \pm 1.6$			T	
RX J1239.4-7502	$-40.7 \pm 2.8$	$-13 \pm 2.4$	$-45.9 \pm 2.8$	$-13.6 \pm 2.6$			T	
CD-69 1055	$-40.9 \pm 2.6$	$-17 \pm 1.1$	$-40.6 \pm 2.1$	$-19.1 \pm 2.0$			T	
MP Mus	$-40.4 \pm 1.0$	$-20 \pm 1.6$	$-40.8 \pm 1.6$	$-23.3 \pm 1.6$			T	
$\eta$ Chamaeleontis cluster								
EG Cha	$-27.1 \pm 1.0$	$25.3 \pm 1.0$	$-29.5 \pm 2.1$	$27.6 \pm 1.6$			T	
HD 75505	$-30.3 \pm 1.4$	$25.0 \pm 1.8$	$-29.9 \pm 2.0$	$27.9 \pm 1.7$			T	

**Notes.**
<sup>a</sup> H=Hipparcos (van Leeuwen 2007); T=Tycho (Høg et al. 1998)

<sup>b</sup> d=discrepant proper motion respect to UCAC3

<sup>c</sup> The 1997 Main Hipparcos Catalogue provides a parallax  $\pi = 15.06$  mas for this object ( $d \sim 66$  pc).

**Fig. 2.** Total proper motion histograms for the different moving groups: Cha I (blue hashed histogram), Cha II (filled red histogram),  $\epsilon$  Cha (green empty histogram),  $\eta$  Cha (orange hashed histogram) and background sources (black dashed-line histogram). Only objects with reliable proper motions are considered.

the rest (see also the discussion in Sect. 6.1). In view of our analysis, we think it unlikely that HD 97048 is actually running away from its birth place.

There is also overall good agreement between the individual parallaxes of the stars in Table 5 and the usually quoted distances

to the associations. The only possible exception is T Cha, whose Hipparcos parallax suggests a greater distance. However, given the large error, this estimation is still consistent with membership to the  $\epsilon$  Cha cluster (but see also discussion in Sect. 5).

### 3.3. Radial velocities of the members of the proper motion groups

Figure 4 shows two plots of the radial velocities versus the proper motion components of the stars. With a couple of exceptions, all the objects from the same proper motion group display similar radial velocities, and are therefore clustered in these diagrams. The radial velocity data therefore confirm that there is a physical relationship between these stars. However, given that all the associations have similar mean radial velocities, in the range 10-20 km/s, it is not possible to distinguish between members of the dark clouds and of the foreground associations on the basis of radial velocity alone.

The largest individual deviations from the mean group values are observed for EM Cha in the  $\eta$  Cha cluster ( $V_r = 4.3 \pm 2$  km/s) and GSC 9420-0948 in the  $\epsilon$  Cha cluster ( $V_r = 5 \pm 2$  km/s). The radial velocities of these stars differ by more than  $3\sigma$  from the mean cluster values, which challenges their membership to the quoted associations. We therefore flag these objects in Table 2. Also, T Cha has a reported radial velocity discrepant in more than  $2\sigma$  from the mean value for the  $\epsilon$  Cha association ( $V_r = 20.0 \pm 2.0$  km/s). The discrepancy may be related to the presence of an unresolved companion, as there is indeed one reported in the literature (Huélamo et al. 2011). We discuss this object further in Sect. 5.



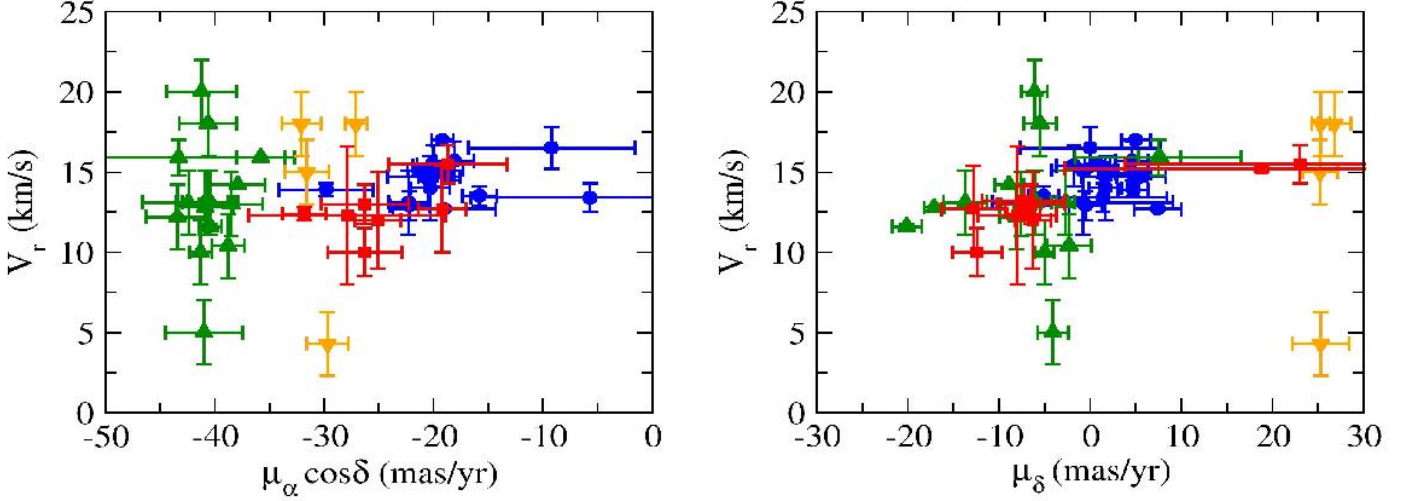


**Fig. 4.** Plots of radial velocity vs. proper motion components for stars in the Chamaeleon associations. Only objects with reliable proper motions are considered. Symbols and colours as in Fig. 1.

**Table 6.** Mean and weighted mean proper motion components and radial velocities for the moving groups identified towards the Chamaeleon sky area<sup>a</sup>

Group	Arithmetic means				Weighted means			
	$\langle \mu_\alpha \cos \delta \rangle$ (mas/yr)	$\langle \mu_\delta \rangle$ (mas/yr)	$\langle \mu \rangle$ (mas/yr)	$\langle V_r \rangle$ (km/s)	$\langle \mu_\alpha \cos \delta \rangle$ (mas/yr)	$\langle \mu_\delta \rangle$ (mas/yr)	$\langle \mu \rangle$ (mas/yr)	$\langle V_r \rangle$ (km/s)
Cha I	$-19.5 \pm 4.8$	$+1.7 \pm 3.9$	$20.0 \pm 4.8$	$14.6 \pm 1.2$	$-20.7 \pm 0.3$	$+0.9 \pm 0.3$	$19.80 \pm 0.12$	$14.02 \pm 0.06$
Cha II	$-23.5 \pm 5.3$	$-7.7 \pm 2.9$	$24.9 \pm 5.3$	$12.9 \pm 1.6$	$-23.9 \pm 0.7$	$-7.8 \pm 0.7$	$25.9 \pm 0.9$	$14.5 \pm 0.2$
$\epsilon$ Cha	$-36.8 \pm 11.7$	$-1.7 \pm 13.2$	$39.8 \pm 9.3$	$13.5 \pm 2.6$	$-37.8 \pm 0.5$	$-1.5 \pm 0.7$	$38.5 \pm 0.5$	$11.7 \pm 0.2$
$\eta$ Cha	$-29.1 \pm 4.9$	$+27.4 \pm 4.9$	$40.4 \pm 3.4$	$17.0 \pm 1.4$	$-29.9 \pm 0.5$	$+25.9 \pm 0.5$	$38.69 \pm 0.03$	$14 \pm 1$

**Notes.**

<sup>a</sup> Interlopers and objects with uncertain proper motion measurements have been excluded from the calculations.

### 3.4. Interlopers

Once the proper motion lists are purged from inaccurate measurements, three true interlopers remain, namely one Chamaeleon I object (2MASS J11183572-7935548) and two Chamaeleon II objects (2MASS J11183572-7935548 and CM Cha), whose proper motions seem to be in better agreement with membership to the  $\epsilon$  Cha group.

The source 2MASS J11183572-7935548 was included as a Chamaeleon I member in the list of Luhman (2007). However, in a later work, Luhman et al. (2008) reclassified it as an  $\epsilon$  Cha member on the basis of its UCAC2 proper motion. Our analysis of the UCAC3 data confirms their result. This object is therefore included in Table 2 as a probable member of the  $\epsilon$  Chamaeleontis cluster.

CM Cha had been listed as a Chamaeleon II member by Spezzi et al. (2008). However, it has UCAC3 proper motion components  $\mu_\alpha \cos \delta = -43.3 \pm 10.6$  and  $\mu_\delta = 7.5 \pm 9.1$  mas/yr. These values are only marginally compatible with the Cha II moving group, and seem to be in better agreement with membership in the foreground  $\epsilon$  Cha association. Unfortunately, AC2000.2 provides no data for this star, and the data provided by SuperCOSMOS are wrong, probably because this object appears blended with other star in the POSS image, so we cannot test its proper motion directly in the way explained above. In the literature we find a reported proper motion of  $(-60, 21)$  mas/yr for this object, with a quoted accuracy of 5-10 mas/yr (Teixeira

et al. 2000). The PPMXL catalogue reports a similar value of  $(-62, 9)$  mas/yr. These measurements are quite discrepant from the UCAC3 measurement, even when the large errors are considered, but indicate in any case that CM Cha is probably located closer to the Sun than the Chamaeleon II members. On the other hand, there is spectroscopic evidence that the object is young: Spezzi et al. (2008) report an equivalent width for the Li I absorption line of  $0.38 \text{ \AA}$ , which is similar to many other cloud members, but close to the lowest values measured by these authors. (Their range encompasses  $0.35$  to  $0.61 \text{ \AA}$ , and typical values in star forming regions are in the range  $0.3$ - $0.8 \text{ \AA}$ .) They also report an H $\alpha$  equivalent width of  $-29 \text{ \AA}$ , which is consistent with low accretion. This suggests that, though young, CM Cha is among the most evolved objects in the Spezzi et al. sample. On the other hand, the reported radial velocity for this star ( $15.9 \pm 1.1$  km/s; Torres et al. (2006) quite well agrees with the values measured for other stars in the Chamaeleon clouds, but also with the radial velocities reported for  $\epsilon$  Cha members (see Sect. 3.3). The space motion of this star (as computed using the UCAC3 proper motions) also seems to be in better agreement with this cluster (see Sect. 5 below). Taking all this into account, we tentatively reclassify CM Cha as a member of the  $\epsilon$  Cha young association, and list it accordingly in Table 2. We note, however, that if the proper motion reported by Teixeira et al. (2000) were correct, this star would probably be located

even closer to the Sun than the  $\epsilon$  Cha members, and thus could be an unrelated young star from the solar neighbourhood.

The situation is also ambiguous for Sz 60W, because the large error in  $\mu_\delta$  makes its UCAC3 proper motion compatible with both the  $\epsilon$  Cha and the Cha II moving groups. This star is part of a binary object with a separation of  $3.6''$ , and the secondary has no UCAC3 counterpart. This may affect the proper motion measurement of the primary, if the system is not completely resolved in the images used by UCAC3 to compute the proper motion, or if source confusion has occurred at some stage. Indeed, secondaries at separations lower than  $10''$  are often not resolved in UCAC3. More precise measurements are required to clarify the nature of Sz 60W, but we note that the spatial location of this source, within the dark cloud (in contrast with CM Cha that is located in the outskirts), suggests a physical connection with Chamaeleon II. For the time being, Sz 60W is listed in Table 1 as a member of this cloud.

In addition, we identify one object, namely CP-68 1388, whose reported UCAC3 proper motion differs from the rest of  $\epsilon$  Chamaeleontis members, and is seen detached from moving group in the vector-point diagram of Fig. 1. This is due to the value of the proper motion in the  $\delta$  direction ( $\mu_\delta = 7.6 \pm 2.3$  mas/yr), because its  $\mu_\alpha \cos \delta$  value ( $-35.8 \pm 2.2$  mas/yr) and its radial velocity (15.9 km/s) are in good agreement with those of other cluster members. This star was observed by Tycho, and the proper motions reported in Table 5 agree closely with the UCAC3 values (although the Tycho  $\mu_\delta$  value is somewhat lower,  $\mu_\delta = 4.70$  mas/yr). The different proper motion and the spatial location of CP-68 1388, to the North of Chamaeleon I and more than  $6^\circ$  away from the closest  $\epsilon$  Chamaeleontis member, makes its membership to the cluster dubious. It is interesting, however, that this object is placed halfway between the  $\epsilon$  and  $\eta$  Chamaeleontis cluster in the vector point diagram. As shown later in Sect. 5, the space velocities of CP-68 1388 agree well with other stars in both clusters. We therefore keep this object in the list of  $\epsilon$  Cha members for the time being.

VW Cha also deserves some comments. This star has been listed in the literature both as a Chamaeleon I member (Luhman 2007) and as a member of the  $\epsilon$  Cha group (Fernández et al. 2008). We find that both its spatial location within the Chamaeleon I southern cloud core and its UCAC3 proper motion ( $\mu_\alpha \cos \delta = -19.7 \pm 1.3$  mas/yr,  $\mu_\delta = -0.8 \pm 3.4$  mas/yr) are in better agreement with VW Cha belonging to the dark cloud. The proper motion values reported by SIMBAD ( $\mu_\alpha \cos \delta = -23$  mas/yr and  $\mu_\delta = -7$  mas/yr; Teixeira et al. (2000) agree well with our classification. This star also has a reported radial velocity ( $V_r = 17.6 \pm 3.3$  km/s; Torres et al. 2006) that is slightly higher than the mean value for Chamaeleon I, but similar to the values reported for other member stars (see Sect. 3.3).

### 3.5. Final member lists

Once the proper motion lists are purged of incorrect measurements, and once the interlopers assigned to the associations they are likely to belong to, the definitive member lists for the Cha I, Cha II,  $\epsilon$  Cha and  $\eta$  Cha contain 73, 22, 21, and 12 stars, respectively. These are the objects presented in Tables 1 and 2. These lists still contain objects with dubious measurements that could not be proved wrong, as discussed in Sect. 3.1.

After this analysis, we computed the means of the proper motion and values for the different kinematic groups, which are listed in Table 6. Interlopers and objects with wrong or dubious proper motion measurements were not considered in the calculations. Because of the large proper motion errors for some of the

objects, we also computed the weighted means, which are also given in Table 6. The values of both the arithmetic and weighted means for each parameter are fully consistent with each other, within the estimated errors.

Table 6 also lists the arithmetic and weighted mean radial velocities that we derive for three of the four groups. For the  $\epsilon$  and  $\eta$  Cha clusters, the mean radial velocities are in good agreement with previously published values (Kharchenko et al. 2005; Wu et al. 2009).

## 4. Proper motions of candidate Chamaeleon members

In the next step, we made an attempt to confirm candidate members of Chamaeleon I and II on the basis of their proper motion. As in our Lupus study, we compared the proper motions of candidate members proposed in the literature with those of the confirmed members.

### 4.1. ROSAT stars

In the 1990s, the ROSAT mission unveiled a dispersed population of X-ray emitting stars towards the Chamaeleon area, but not confined to the dark clouds (Alcalá et al. 1995). Alcalá et al. (1997) provided the first spectroscopic evidence that these stars were young. Covino et al. (1997) performed radial velocity measurements for most of these stars, showing that the sample included objects belonging to different kinematical populations. This result was confirmed for a subsample of these objects by Frink et al. (1998) combining information from several proper motion catalogues. In addition, these authors used the Hipparcos parallaxes available for some of the stars to show that they were located at different distances (from 60 to about 200 pc). The different stellar populations identified by these authors were thus assigned to the Chamaeleon I cloud, the foreground  $\epsilon$  Cha cluster, or to an undetermined field population. However, many stars remained unclassified owing to the lack of proper motions. Only 18 out of the 81 stars studied by Covino et al. (1997) are included in our compilations of members of the associations seen towards the Chamaeleon area. These objects are flagged in Tables 1 and 2.

To clarify the nature of the remaining ROSAT sources, we performed the same proper motion analysis on them described in Sect. 3.1. UCAC3 provides proper motion measurements for 38 of these objects, listed in Table 7. The radial velocities and evolutionary status of these stars according to Covino et al. (1997) are also indicated. We show the vector point diagram for these objects in Fig. 5, compared to the loci of the known young populations in the Chamaeleon area. We also show the spatial location of the ROSAT sources in Fig. 3.

The UCAC3 vector point diagram confirms that the ROSAT stars are a mixture of different kinematical populations. From their position on this diagram, some sources present completely discrepant proper motions from any of the moving groups identified in Sect. 3.1. The radial velocity measurements from Covino et al. (1997) confirm that these stars follow a completely different motion pattern with respect to the Chamaeleon associations. Other sources can be nicely assigned to one of the moving groups in the Chamaeleon sky area; however, a few of them are also discarded because their radial velocities, as provided by Covino et al. (1997), are in complete disagreement with membership to any of the associations, or because their location in the sky does not coincide with that of the group with similar



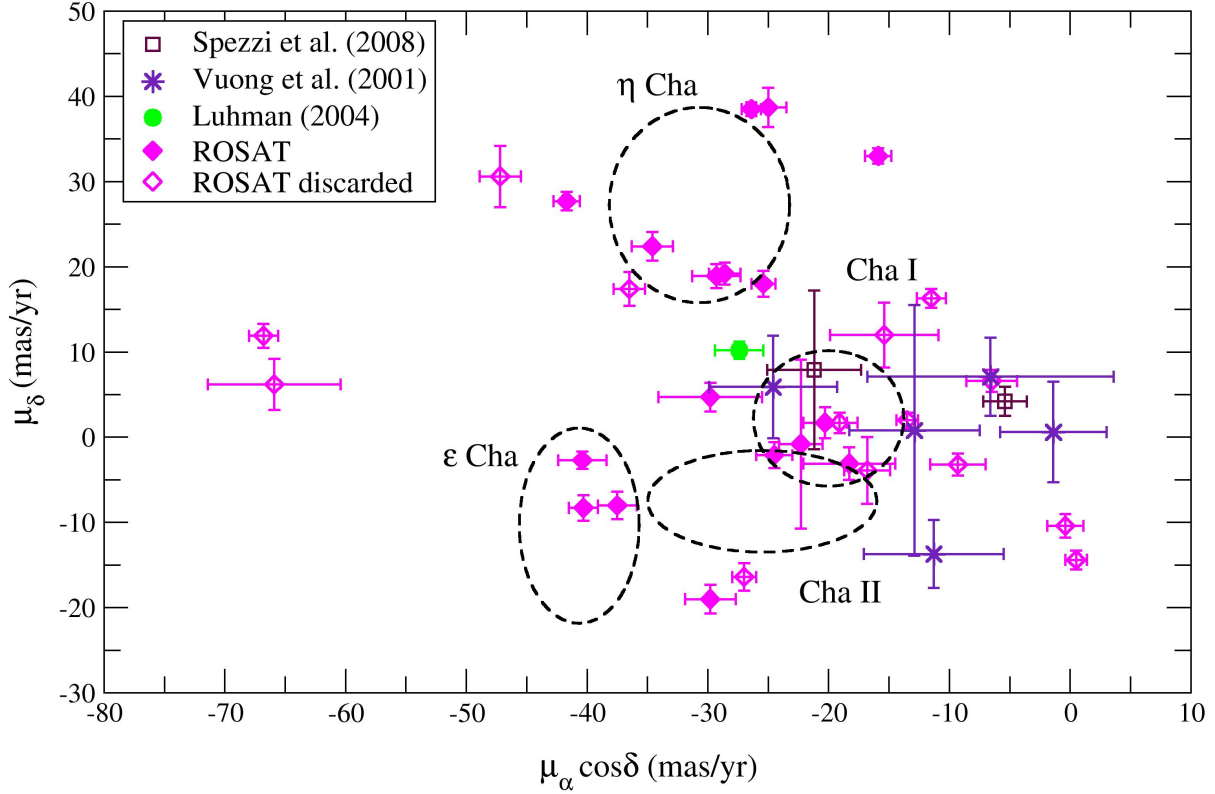


**Fig. 5.** Vector point diagram for Chamaeleon candidate members from the literature. The ellipses indicate the approximate location of the kinematical groups identified in Fig. 1.

proper motion (especially in the case of the dark clouds). All the ROSAT objects with discrepant proper motions and/or radial velocities are classified as zero-age main sequence (ZAMS) stars or stars of unclear nature by these authors.

This left us with 13 stars (11 PMS stars and two stars of unclear nature) whose spatial location, proper motions and radial velocities (except for RXJ1150.4-7704, which has no available radial velocity measurement) all overlap with one of the Chamaeleon moving groups. We assigned two of these objects to the Cha I moving group. The eleven other sources are classified as candidate members of the  $\epsilon$  Cha association (three objects) or the  $\eta$  Cha association (eight objects). We do not find any good Chamaeleon II candidate members. The membership of all these sources is indicated in Table 7.

In two cases, namely RXJ1123.2-7924 and RX J1158.5-7913, membership in a single association cannot be clearly attributed. The spatial location of these two objects (two PMS stars according to the study by Covino et al. (1997) seems more consistent with membership in the  $\epsilon$  Cha moving group than in either of the dark clouds. However, this is not so straightforward from their UCAC3 proper motions. RXJ1123.2-7924 is located in the vector point diagram closer to the Cha II moving group than to the  $\epsilon$  Cha members, but its proper motion values are still marginally consistent with membership in this group. Given its location in the sky, in the area between the Chamaeleon I and the Chamaeleon III clouds, and about  $5^\circ$  from the known

Chamaeleon II members, we tentatively assign this object to the  $\epsilon$  Cha moving group, and list it in Table 7.

RX J1158.5-7913 is seen towards the small cloud [DB2002b] G300.23-16.89, located halfway between the Chamaeleon I and II clouds and about  $2.8^\circ$  south-east of the former. The star T Cha and other members and candidate members of the  $\epsilon$  Cha association are also seen in this area. However, the proper motion components of RX J1158.5-7913 ( $\mu_\alpha \cos \delta = -18.3 \pm 3.8$  mas/yr,  $\mu_\delta = -3.1 \pm 1.9$  mas/yr) place this star in the overlapping area between Chamaeleon I and II members in the vector point diagram, but closer to the Chamaeleon I mean value given in Table 6. This looks completely incompatible with membership in the  $\epsilon$  Cha cluster, even though the radial velocity reported by Covino et al. ( $V = 13.1 \pm 2$  km/s) is very close to the mean value we obtain for the  $\epsilon$  Cha members (see Table 6). Because the proper motion and radial velocity look consistent with the mean values derived for the Cha I moving group, we tentatively assign RX J1158.5-7913 to this cloud for the time being. More accurate kinematic data will help clarify the nature of this object.

#### 4.2. Other candidate members from the literature

Several works have provided lists of candidate members in the Chamaeleon clouds that still lack spectroscopic confirmation of youth. Unfortunately, most of the postulated objects are too faint

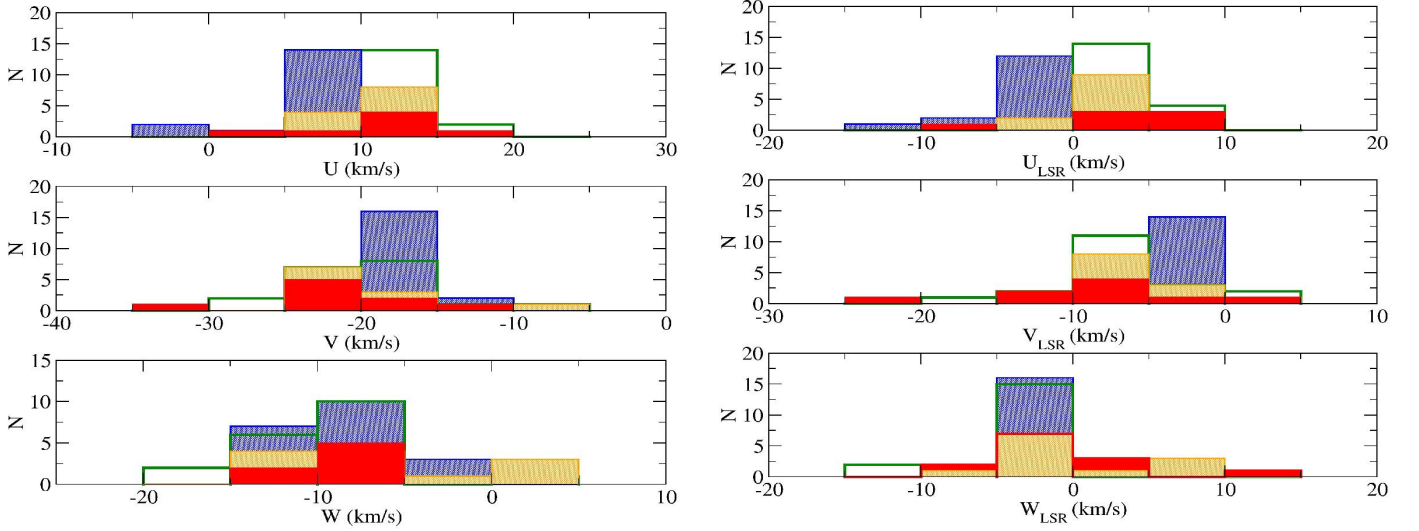


**Fig. 6.** Histograms of space velocities, uncorrected and corrected for the solar reflex motion with respect to the LSR (left and right panels, respectively) for stars in the different Chamaeleon associations. Symbols as in Fig. 2.

to be included in the UCAC3 catalogue and, therefore, we cannot test their membership on the basis of their proper motion. There are, however, a few exceptions, which we discuss in this section. The UCAC3 proper motions for these candidates are listed in Table 8, and they are plotted in the vector point diagram shown in Fig. 5.

Luhman et al. (2004) provides a list of objects whose membership in Chamaeleon I is uncertain (cf. his Table 8), 21 of them lacking confirmation in later works. Only one of these objects has a valid UCAC3 counterpart, namely C1-14, an infrared source first quoted by Prusti et al. (1991), and also identified with the X-ray source CHX 15a.<sup>6</sup> This object is located within the northern cloud core of Chamaeleon I and, as shown in Fig. 5, its proper motion is compatible with the Cha I moving group. The spectral type of this source is badly constrained, but quoted in the range F0-A7, which would make it one of the most massive objects in the dark cloud, together with HD 97300 and HD 97048.

In addition to the confirmed Chamaeleon II members, Spezzi et al. (2008) list a number of objects still lacking spectroscopic confirmation of membership to the cloud, but considered likely members on the basis of the multiwavelength photometric analysis reported in a previous work (Alcalá et al. 2008). Only two of these sources have UCAC3 counterparts, namely IRAS 12589-7646 (ISO-Cha II 89) and IRAS 12448-7650. The proper motion for the latter object clearly disagrees with membership in the Cha II moving group, and strongly suggests that IRAS 12448-7650 belongs to the background. As for IRAS 12589-7646, its proper motion ( $\mu_\alpha \cos \delta = -21.2 \pm 3.9$  mas/yr,  $\mu_\delta = 7.9 \pm 3.9$  mas/yr) places this source in the area of the Cha I moving group rather than Cha II. From our own check, however, the proper motion seems to be around (5, 1.1) mas/yr, which would place it in the same area as the background objects in the vector-point diagram. In view of these results, the classification of IRAS 12589-7646 as a Chamaeleon II member is dubious, and we conservatively flag it as “rejected” in Table 8.

<sup>6</sup> In addition to C1-14, SIMBAD lists three other sources within 2'' (the value of our cross-matching radius) from the UCAC3 position: CD-75 522, Glass R, and WKK F 32. The former has a reported proper motion suggesting it is a foreground star. From the intercomparison of their properties as listed in SIMBAD, we are led to think that Glass R, WKK F 32, and C1-14 must actually be the same object.

Vuong et al. (2001) performed a search for candidate members of Chamaeleon II based on DENIS *IJKs* photometry. Only five objects from their list are included in UCAC3, namely their sources [VCE2001] C18, C29, C64, X3, and X4. As seen in Fig. 5, their proper motions do not agree with membership in the Cha II moving group. Therefore, it seems unlikely that these objects belong to the Chamaeleon II dark cloud. The only possible exception is the X-ray source [VCE2001] X4, whose location in the vector point diagram is marginally compatible with those of the Chamaeleon II members. While deceiving, this result is not totally surprising, since spectroscopic studies of about 30 sources from the Vuong et al. (2001) selection also failed to confirm most of them as Chamaeleon II members (Barrado y Navascués & Jayawardhana 2004; Spezzi et al. 2008), thus showing the high contamination of the original sample (which amounted to 76 sources). None of the five DENIS sources discussed above with available proper motions was observed in these works. To date, there have only been five confirmed young stars from the Vuong et al. (2001) list (see compiled list in Spezzi et al. 2008), but only one, [VCE2001] C61, is included in UCAC3 and listed in Table 1. The proper motion of this object is compatible with Chamaeleon II membership.

## 5. Space velocities

We computed the galactic space velocities for the stars (members and candidate members) with available radial velocity measurements. For this purpose we made use of an IDL routine retrieved from the IDL Astronomy Library,<sup>7</sup> originally written by W. Landsman and later modified by S. Koposov. The procedure follows the formulation in Johnson & Soderblom (1987), except for two details: the *U* component is positive toward the Galactic anticentre, and the Hipparcos transformation matrix is used. We modified the routine to include the computation of the velocity errors in the way prescribed by Johnson & Soderblom (1987).

Since most of the stars lack parallax measurements, we assumed the canonical distances to the associations for this calculation:  $160 \pm 15$  pc and  $178 \pm 18$  pc to Chamaeleon I and II, respectively (Whittet et al. 1997), and  $111 \pm 5$  pc and  $97 \pm 5$  pc to the  $\epsilon$  Cha and  $\eta$  Cha clusters, respectively (Feigelson et al.

<sup>7</sup> [http://idlastro.gsfc.nasa.gov/ftp/pro/astro/gal\\_uvw.pro](http://idlastro.gsfc.nasa.gov/ftp/pro/astro/gal_uvw.pro)

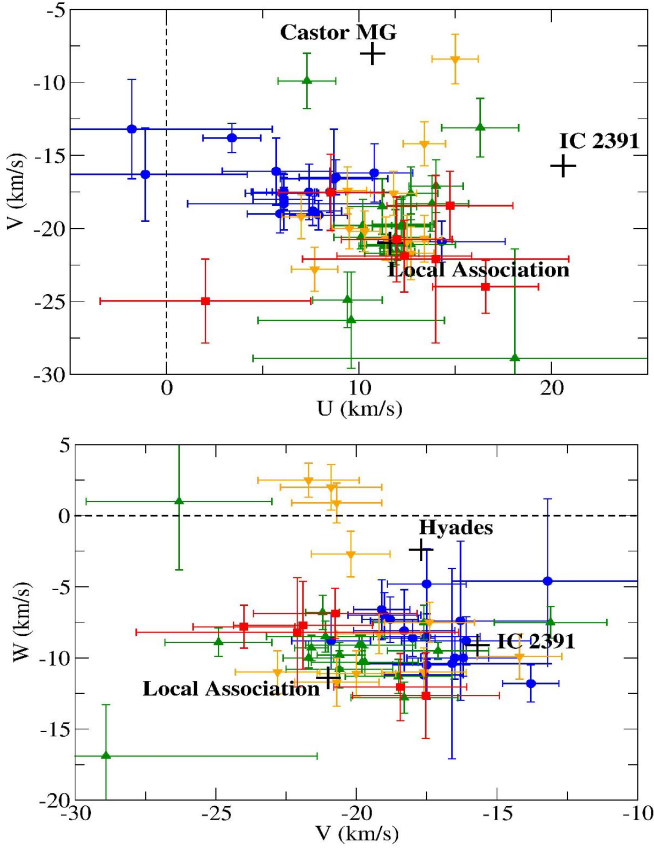


**Fig. 7.**  $(U, V)$  and  $(V, W)$  planes for stars in the different Chamaeleon association. The big crosses indicate the location of known nearby moving groups. Rest of symbols and colours as in Fig. 1.

2003). For T Cha and CV Cha, we used the distances inferred from their Hipparcos parallaxes as given in Table 5.

The resulting space velocities are listed in Table 9, as well as the velocities corrected for the velocity of the Sun with respect to the local standard of rest (LSR), assumed to be  $(U_{\odot}, V_{\odot}, W_{\odot}) = (-8.5, 13.38, 6.49)$  km/s. Figure 6 shows the histograms for the space velocities of the stars in the different associations.

Although this exercise is certainly affected by lots of uncertainties, especially in the stellar distances, the resulting space velocities confirm the membership of the stars in the different Chamaeleon associations to the young disk population, according to the prescriptions listed in Leggett (1992). The histograms displayed in Fig. 6 further confirm the presence of different kinematical populations towards Chamaeleon. In particular, the stars in the Chamaeleon I cloud seem to display, as a sample, a different motion pattern from the rest. This is most evident in the Galactic centre-anticentre direction ( $U$  component), especially when the velocities are corrected with respect to the LSR (upper right panel of Fig. 6): While the mean  $U_{LSR}$ -component of the Cha I moving group is negative (i.e. pointing to the Galactic centre), for the rest of associations this component is positive (i.e. pointing to the Galactic anticentre).

The stars in the two foreground clusters seem to have very similar space velocities, so the differences in proper motion observed in the vector point diagram of Fig. 1 seem to be mostly related to the different spatial location of both groups in the projected sky (separated by about  $8.5^\circ$ ). This fact, together with the similar ages and distances of both associations, hints at a con-

nection between them, as already suggested in the literature (e.g. Feigelson et al. 2003). Indeed, the space velocities we obtain are in good agreement with published values (e.g. Zuckerman & Song 2004), and with the membership of both clusters to the so-called “Local Association” (or “Pleiades moving group”), a coherent kinematic stream of young stars (ages  $\sim 20$ – $150$  Myr) with embedded clusters and associations (such as the Pleiades,  $\alpha$  Per or Scorpius-Centaurus) first postulated by Eggen (1975). This is shown in Fig. 7, where we show the location of the stars from Table 9 in the  $(U, V)$  and  $(V, W)$  planes, together with the location of the mean space velocities for several nearby young moving groups (ages 20–600 Myr; Montes et al. 2001).

Interestingly, the stars in Chamaeleon II seem to have space velocities more similar to those of the foreground clusters than to the Chamaeleon I stars. However, the numbers are low, and the errors for most stars are large, as is the dispersion in the data. Better precision and statistics with larger samples are required to investigate the eventual relation of Chamaeleon II with the  $\epsilon$  and  $\eta$  Cha associations, and to other young moving groups.

We close this section with some remarks on particular objects. First of all, we note that the usually quoted parallax for T Cha is  $15 \pm 3$  mas, corresponding to a distance of only  $66 \pm 15$  pc. This is the value included in the Hipparcos Main Catalogue (ESA 1997). However, the new reduction performed by (van Leeuwen 2007) provides a parallax of  $6 \pm 3$  mas, corresponding to a distance of  $160 \pm 80$  pc. The first value would place this star closer to the Sun than most of the members of the  $\epsilon$  Cha association, and with quite discrepant space velocities, even when the errors are considered. In contrast, the most recent distance value is compatible, within the error, with the canonical distance to the cluster, and provides space velocities in relatively good agreement with T Cha being an  $\epsilon$  Cha member. The same trend is observed if the space velocities are computed using the Hipparcos proper motions from Table 5 instead of the UCAC3 ones. Nevertheless, T Cha is seen detached from the group of  $\epsilon$  Cha members in both planes represented in Fig. 7, and, given the large uncertainties in the distance (i.e. in the space velocities), the membership of this star to the  $\epsilon$  Cha moving group cannot be assigned with certainty.

Second, we note that the space velocities of CM Cha show relatively good agreement with those of other  $\epsilon$  Cha members, when the mean distance to this cluster is used in the calculation. If the distance to Chamaeleon II is used instead, the resulting space velocities are quite discrepant from those of the only confirmed Cha II member with available space velocities. This further supports the hypothesis that CM Cha is a member of the  $\epsilon$  Cha association, as suggested in Sect. 3.4. Even so, it must be noted that the velocity component in the direction of the Galactic poles ( $W$ ) of CM Cha is quite different from the rest of  $\epsilon$  Cha members, as it is pointing towards the northern instead of the southern Galactic pole. We note, though, that a handful of  $\eta$  Cha cluster members are also located in the same area of the  $(V, W)$  plane.

We made the same check with the two ROSAT sources discussed at the end of Sect. 4.1. RX J1158.5-7913, a potential interloper from the Chamaeleon I cloud in the sky area of the  $\epsilon$  Cha members, has space velocities that are fully consistent with membership in the dark cloud, if the mean distance to it is used in the calculation. In contrast, the resulting space velocities when the distance to  $\epsilon$  Cha is used are not consistent with membership in this cluster. On the other hand, RXJ1123.2-7924, whose proper motion looks compatible with both the  $\epsilon$  Cha cluster and the Chamaeleon II cloud, has space velocities fully compatible with the foreground association.

## 6. Properties of the kinematic populations of the Chamaeleon dark clouds

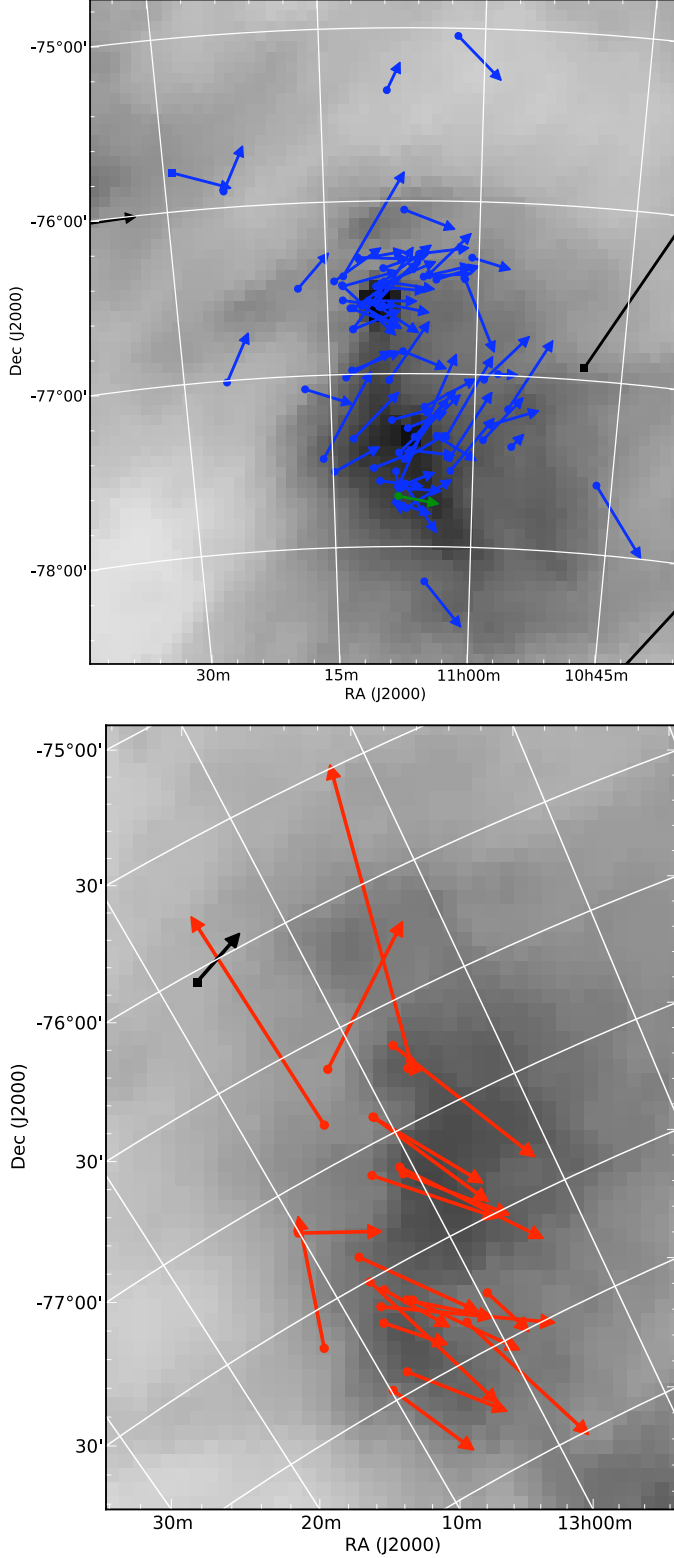


**Fig. 8.** Enlargements of the map from Fig. 3 showing the Chamaeleon I and II areas in more detail (upper and lower panels, respectively).

### 6.1. Spatial location

Figure 8 shows two enlargements of Fig. 3 in the location of the Chamaeleon I and II clouds. As noted in previous works, the sources belonging to the Cha I moving group tend to cluster around the two main cores containing the intermediate-mass stars HD 97300 (the northern core) and HD 97048 (the southern core). Luhman (2007) reports on a difference in isochronal ages of a few Myr between both cores, which he interprets as the result of two different bursts of star formation. We therefore checked whether any proper motion difference could be seen between the two cores. To this purpose, all the stars within a radius of  $50'$  from one of the intermediate-mass star were defined as members of the corresponding core. This distance was chosen after inspecting the distance distributions from both intermediate-mass stars. At the UCAC3 precision, we found no obvious difference between the proper motions of both groups.

No evident difference is seen either between the in- and the off-cloud populations, neither in proper motion moduli nor in proper motion directions. This seems to confirm that both samples belong to the same structure. It also suggests that the location of the outer sources is not the consequence of these objects being ejected from their parental birth sites.

We performed a similar analysis in Chamaeleon II, dividing the population in a northern group, located north-west of a dense core in the northern part of the cloud, and a southern group, located in and around a smallest core to the south. Again, we found no obvious difference between the proper motions of both groups. A comparison between the in- and off-cloud population is not possible in this case due to the low number of objects and the dubious proper motions of most of the sources located off-cloud (leftmost sources in the lower panel of Fig. 8).

### 6.2. Physical parameters

As a next step, we investigated the possible correlations between the proper motions and the physical parameters of the objects. Luhman et al. (2008) performed an analysis of the spectral energy distributions (SEDs) of confirmed members of Chamaeleon I. A similar study of Chamaeleon II was presented by Alcalá et al. (2008) and Spezzi et al. (2008). These works provide a classification of the confirmed members of the dark clouds into class III (diskless) sources, class II (disk) sources and so-called “flat-spectrum sources”, which are thought to be halfway between class I (envelope) sources and class II sources. They also provide estimations of the effective temperature and bolometric luminosity of the objects. In total, we compiled values of physical parameters for 47 stars in Cha I and 14 stars in Cha II, whose properties are summarized in Table 10. Only objects with reliable UCAC3 proper motions are included.

We used this information to look for correlations between the proper motions and the physical parameters of the objects. Figures 9 and 10 show the plots of the proper motion components versus  $T_{eff}$  and  $\log L/L_{\odot}$  for the objects in both clouds. No trends are seen in the proper motion with either of the considered parameters. Since these properties are directly correlated with mass in young low-mass stars, this result suggests that the motion of the objects does not depend on their mass to the precision that we can prove with the UCAC3 data.

In Chamaeleon I, where this can be investigated, we do not find any correlation either between proper motion and the presence of a (primordial) circumstellar disk, or for objects with and without disks (class II and class III sources) separately.



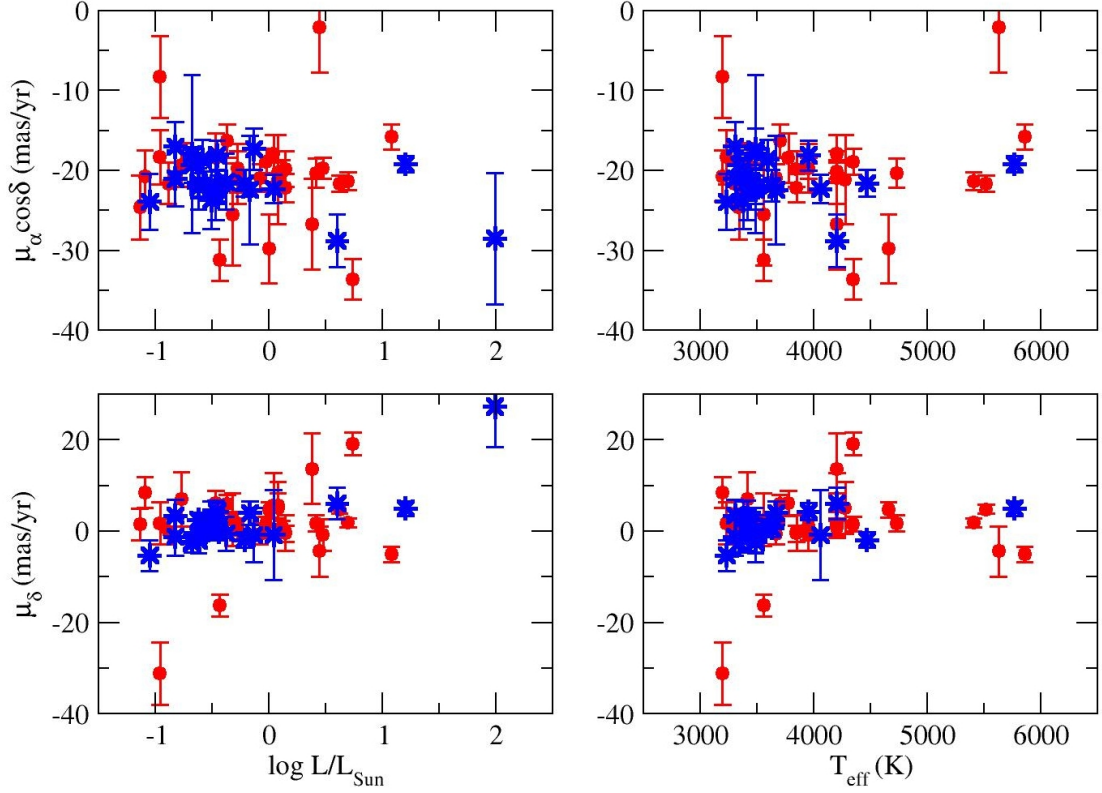


**Fig. 9.** Proper motion components versus bolometric luminosity (left) and effective temperature (right) for Chamaeleon I members with and without disks (red circles and blue asterisks, respectively).

We note that similar studies in other star-forming regions also failed to find any correlation between the proper motion and the properties of the objects (e.g. Bouy & Martín 2009, LSJ11). More accurate proper motion measurements and better statistics are required to reveal any eventual trend with the physical properties of young low-mass stars in these regions.

## 7. Conclusions

We have performed a kinematic study of the Chamaeleon clouds based on UCAC3 proper motions and radial velocities from the literature. Our analysis has led to the following conclusions:

- With the UCAC3 data, we were able to separate the several distinct kinematic groups that coexist in the Chamaeleon sky area: the Chamaeleon I and II dark clouds, the young  $\epsilon$  Cha and  $\eta$  Cha associations, and the field contaminants.
- Compiled radial velocity data from the literature showed that all the young stars have similar radial velocities, regardless of the association the objects belong to. It is not possible to discern membership to the different groups seen towards Chamaeleon on the basis of radial velocity information alone.
- The stars in Chamaeleon I and II may have different kinematical properties, but this result must be confirmed with more precise proper motions. If true, the Chamaeleon II members would be moving faster in the tangential direction than the Chamaeleon I members. Because they are located at the same or a further distance, this would question the physical connection between both clouds.
- The kinematical analysis confirmed the membership of almost all the studied objects to the corresponding associa-

tions. We only identified two possible interlopers from the  $\epsilon$  Cha association in our list of Chamaeleon II members: CM Cha and Sz 60W. With the available data, we reclassified CM Cha as an  $\epsilon$  Cha member. The nature of Sz 60W is more uncertain due to the big proper motion error, but given its spatial location and its isochronal age (2 Myr) we think it more likely that this object belongs to Chamaeleon II.

- We reanalysed a sample of X-ray detected stars towards the Chamaeleon sky area and confirmed that they constitute a mixture of different populations. After purging the sample of foreground and background contaminants and excluding the objects previously classified in the literature, we identified two stars as likely Chamaeleon I members, three as  $\epsilon$  Cha members, and eight as  $\eta$  Cha members. We did not identify any Chamaeleon II members in this sample.
- We checked the proper motions of candidate members of the Chamaeleon dark clouds from the literature, and confirmed one object, C1-14, as a probable member of Chamaeleon I. This would be one of the earliest type (i.e. most massive) stars in this dark cloud. In Chamaeleon II, we checked the proper motions of two candidate members listed by Spezzi et al. (2008) and of five candidate members from the list by Vuong et al. (2001), and found it unlikely that any of them belongs to the dark cloud.
- For those objects with available radial velocities, we computed the corresponding Galactic space motions. Our results confirm the different spatial motion of Chamaeleon I from the foreground associations. The data also hint at a difference in spatial motion between Chamaeleon I and II, further suggesting different origins for the populations in both clouds, but this has to be confirmed with better datasets.

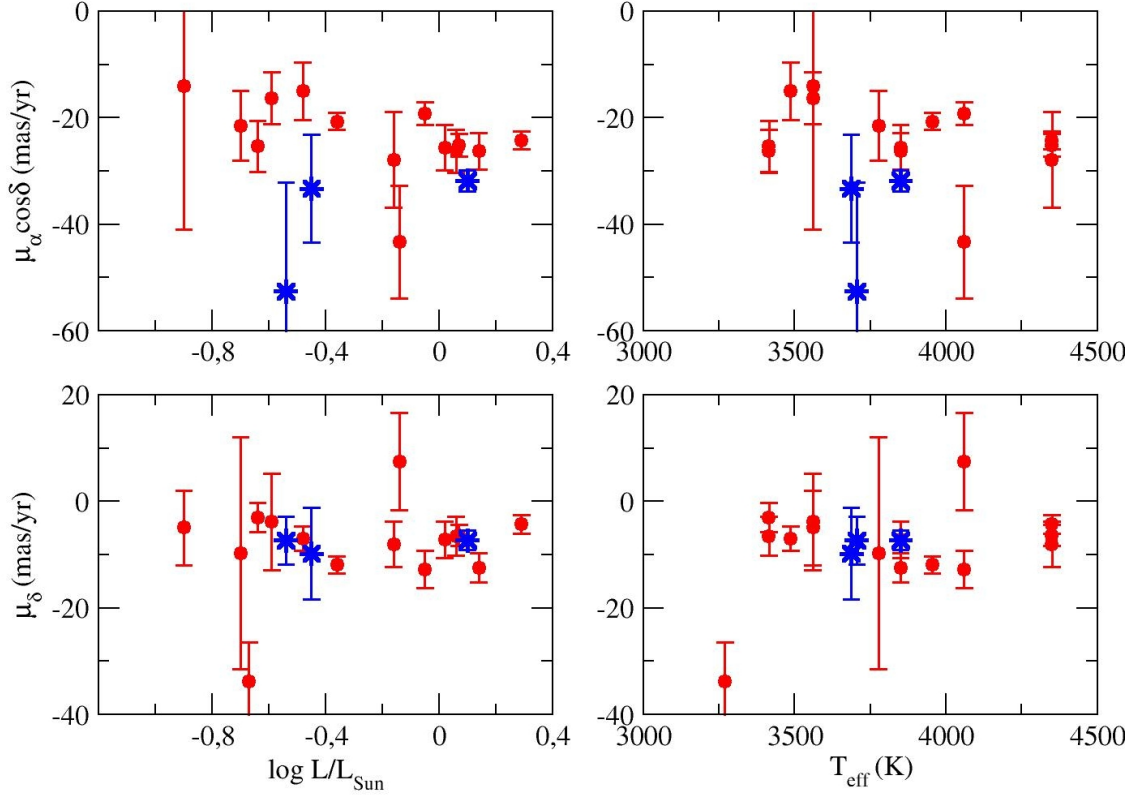


**Fig. 10.** Same as Fig. 9 for Chamaeleon II.

- The space velocities for the  $\epsilon$  and  $\eta$  Cha members and candidate members are in very good agreement with previous estimations in the literature, which identify these two clusters as part of the Local Association. Interestingly, the space motions of most of the Cha II members with available radial velocity measurements also look quite similar to those of the Local Association stars. It would be highly desirable to have a larger sample of stars with estimated space velocities in this dark cloud, in order to investigate the eventual relation between Chamaeleon II and the Local Association and to confirm or discard the different motion pattern from Chamaeleon I.
- We investigated the relation between the proper motions and the published properties of the members and candidate members of Chamaeleon I and II, such as spatial location, the presence of circumstellar material, effective temperature, or luminosity, but we found no evident correlations. More accurate proper motions, combined with radial velocity information, may unveil possible hidden trends with the physical properties of the stars, undetectable with the precision of the proper motions used here.

Our work has shown how the use of kinematical information can complement photometric and spectroscopic data to constrain the selection of members of young star-forming clusters, minimizing the contamination of the samples. Currently available astrometric catalogues are deep enough to provide proper motions for a significant number of candidate members of nearby star-forming regions precisely enough to disentangle true members, not only from background sources, but also from young stars in clusters overlapping in the line of sight. In a forthcoming paper (López Martí et al. in preparation), we will report on a search

for new candidate members of the Chamaeleon clouds based on proper motion.

Furthermore, the results obtained both in the present work and in our previous Lupus study illustrate the potential of using a VO methodology for analysing heterogeneous datasets in an efficient manner.

Most of the issues left unsolved in the present study are expected to get a definitive answer with the advent of the *Gaia* mission of the European Space Agency, whose launch is foreseen in 2013. *Gaia* will provide astrometric information with unprecedented precision for most of the stars in the samples studied here, remarkably improving our understanding of the kinematics, physical properties and formation process of the objects in the Chamaeleon associations.

**Acknowledgements.** This work was funded by the Spanish MICINN through grant Consolider-CSD2006-00070. It also benefitted from funding from the Spanish government through grants ESP2007-65475-C02-02, AYA2008-02156, AYA2010-21161-C02-02, and AyA2011-24052, and from the Madrid regional government through grant PRICIT-S2009ESP-1496. A. B. was co-funded under the Marie Curie Actions of the European Commission (FP7-COFUND).

This publication made use of VOSA, developed under the Spanish Virtual Observatory project supported by the Spanish MEC through grants AyA2008-02156 and AyA2011-24052. It greatly benefitted from the use of the SIMBAD database and the VIZIER Catalogue Service, both operated at the CDS (Strasbourg, France). We used the VO-compliant tools Aladin, developed at the CDS, and TOPCAT, currently developed within the AstroGrid project.

This publication makes use of data products from the Two Micron All Sky Survey (2MASS), which is a joint project of the University of Massachusetts and the Infrared Processing and Analysis Center/California Institute of Technology, funded by the US National Aeronautics and Space Administration and National Science Foundation, and from the Wide-field Infrared Survey Explorer (WISE), which is a joint project of the University of California, Los Angeles, and the Jet Propulsion Laboratory/California Institute of Technology, funded by the US National Aeronautics and Space Administration.



## References

- Alcalá, J. M., Krautter, J., Covino, E., et al. 1997, *A&A*, 319, 184
- Alcalá, J. M., Krautter, J., Schmitt, J. H. M. M., et al. 1995, *A&A*, 114, 109
- Alcalá, J. M., Spezzi, L., Chapman, N., et al. 2008, *ApJ*, 676, 427
- Barrado y Navascués, D. & Jayawardhana, R. 2004, *ApJ*, 615, 840
- Bate, M. R. 2012, *MNRAS*, 419, 3115
- Bate, M. R., Bonnell, I. A., & Bromm, V. 2003, *MNRAS*, 339, 577
- Bayo, A., Rodrigo, C., Barrado, D., et al. submitted, *A&A*
- Bayo, A., Rodrigo, C., Barrado y Navascués, D., et al. 2008, *A&A*, 492, 277
- Bianchi, L. & GALEX Team. 2000, *Mem. Soc. Astron. Italiana*, 71, 1123
- Biazio, K., Alcalá, J. M., Covino, E., et al. 2012, *A&A*, 547, A104
- Bouy, H. & Martín, E. L. 2009, *A&A*, 504, 981
- Caballero, J. A. 2010, *A&A*, 514, A18
- Covino, E., Alcalá, J. M., Allain, S., et al. 1997, *A&A*, 328, 187
- Cutri, R. M. & et al. 2012, *VizieR Online Data Catalog*, 2311, 0
- da Silva, L., Torres, C. A. O., de La Reza, R., et al. 2009, *A&A*, 508, 833
- DENIS Consortium. 2005, *VizieR Online Data Catalog*, 2263, 0
- Dubath, P., Reipurth, B., & Mayor, M. 1996, *A&A*, 308, 107
- Eggen, O. J. 1975, *PASP*, 87, 37
- Evans, II, N. J., Allen, L. E., Blake, G. A., et al. 2003, *PASP*, 115, 965
- Feigelson, E. D., Lawson, W. A., & Garmire, G. P. 2003, *ApJ*, 599, 1207
- Fernández, D., Figueras, F., & Torra, J. 2008, *A&A*, 480, 735
- Frink, S., Roeser, S., Alcalá, J. M., Covino, E., & Brandner, W. 1998, *A&A*, 338, 442
- Gauvin, L. S. & Strom, K. M. 1992, *ApJ*, 385, 217
- Hambly, N. C., MacGillivray, H. T., Read, M. A., et al. 2001, *MNRAS*, 326, 1279
- Hauck, B. & Mermilliod, M. 1998, *A&AS*, 129, 431
- Helou, G. & Walker, D. W., eds. 1988, *Infrared astronomical satellite (IRAS) catalogs and atlases. Volume 7: The small scale structure catalog, Vol. 7*
- Høg, E., Fabricius, C., Makarov, V. V., et al. 2000, *A&A*, 355, L27
- Høg, E., Kuzmin, A., Bastian, U., et al. 1998, *A&A*, 335, L65
- Huélamo, N., Lacour, S., Tuthill, P., et al. 2011, *A&A*, 528, L7
- Hughes, J. & Hartigan, P. 1992, *AJ*, 104, 680
- Ishihara, D., Onaka, T., Katata, H., et al. 2010, *A&A*, 514, A1
- Jeffries, R. D., Maxted, P. F. L., Oliveira, J. M., & Naylor, T. 2006, *MNRAS*, 371, L6
- Joergens, V. 2006, *A&A*, 448, 655
- Joergens, V. & Guenther, E. 2001, *A&A*, 379, L9
- Johnson, D. R. H. & Soderblom, D. R. 1987, *AJ*, 93, 864
- Kharchenko, N. V., Piskunov, A. E., Röser, S., Schilbach, E., & Scholz, R.-D. 2005, *A&A*, 438, 1163
- Kraus, A. L. & Hillenbrand, L. A. 2007, *ApJ*, 662, 431
- Kroupa, P. & Bouvier, J. 2003, *MNRAS*, 346, 369
- Leggett, S. K. 1992, *ApJS*, 82, 351
- López Martí, B., Eislöffel, J., Scholz, A., & Mundt, R. 2004, *A&A*, 416, 555
- López Martí, B., Jiménez-Esteban, F., Bayo, A., et al. in preparation, *A&A*
- López Martí, B., Jiménez-Esteban, F., & Solano, E. 2011, *A&A*, 529, A108
- Luhman, K. L. 2004, *ApJ*, 602, 816
- Luhman, K. L. 2007, *ApJS*, 173, 104
- Luhman, K. L. 2008, in *Handbook of Star Forming Regions, Volume II: The Southern Sky*, ed. B. Reipurth, 169
- Luhman, K. L., Allen, L. E., Allen, P. R., et al. 2008, *ApJ*, 675, 1375
- Luhman, K. L. & Muench, A. A. 2008a, *ApJ*, 684, 654
- Luhman, K. L. & Muench, A. A. 2008b, *ApJ*, 684, 654
- Luhman, K. L., Peterson, D. E., & Megeath, S. T. 2004, *ApJ*, 617, 565
- Luhman, K. L. & Steeghs, D. 2004, *ApJ*, 609, 917
- Mamajek, E. E., Lawson, W. A., & Feigelson, E. D. 1999, *ApJ*, 516, 77
- Maxted, P. F. L., Jeffries, R. D., Oliveira, J. M., Naylor, T., & Jackson, R. J. 2008, *MNRAS*, 385, 2210
- Mermilliod, J.-C. & Mermilliod, M. 1994, *Catalogue of Mean UBV Data on Stars*
- Monet, D. G., Levine, S. E., Canzian, B., et al. 2003, *AJ*, 125, 984
- Montes, D., López-Santiago, J., Gálvez, M. C., et al. 2001, *MNRAS*, 328, 45
- Morau, E., Bouvier, J., & Stauffer, J. R. 2001, *A&A*, 367, 211
- Ochsenbein, F., Bauer, P., & Marcout, J. 2000, *A&AS*, 143, 23
- Prusti, T., Clark, F. O., Whittet, D. C. B., Laureijs, R. J., & Zhang, C. Y. 1991, *MNRAS*, 251, 303
- Röser, S., Demleitner, M., & Schilbach, E. 2010, *AJ*, 139, 2440
- Röser, S., Schilbach, E., Schwan, H., et al. 2008, *A&A*, 488, 401
- Sartori, M. J., Lépine, J. R. D., & Dias, W. S. 2003, *A&A*, 404, 913
- Schlegel, D. J., Finkbeiner, D. P., & Davis, M. 1998, *ApJ*, 500, 525
- Schwartz, R. D. 1977, *ApJS*, 35, 161
- Schwartz, R. D., Wilking, B. A., & Giubudagian, A. L. 1991, *ApJ*, 370, 2635
- Skrutskie, M. F., Cutri, R. M., Stiening, R., et al. 2006, *AJ*, 131, 1163
- Spezzi, L., Alcalá, J. M., Covino, E., et al. 2008, *ApJ*, 680, 1295
- Spezzi, L., Alcalá, J. M., Frasca, A., Covino, E., & Gandolfi, D. 2007, *A&A*, 470, 281
- Teixeira, R., Ducourant, C., Sartori, M. J., et al. 2000, *A&A*, 361, 1143
- Tetzlaff, N., Neuhäuser, R., & Hohle, M. M. 2011, *MNRAS*, 410, 190
- Torres, C. A. O., Quast, G. R., da Silva, L., et al. 2006, *A&A*, 460, 695
- Urban, S. E., Corbin, T. E., & Wycoff, G. L. 1998, *AJ*, 115, 2161
- van Leeuwen, F. 2007, *A&A*, 474, 653
- Vuong, M. H., Cambrésy, L., & Epchtein, N. 2001, *A&A*, 379, 208
- Whittet, D. C. B., Prusti, T., Franco, G. A. P., et al. 1997, *A&A*, 327, 1194
- Wright, E. L., Eisenhardt, P. R. M., Mainzer, A. K., et al. 2010, *AJ*, 140, 1868
- Wu, Z.-Y., Zhou, X., Ma, J., & Du, C.-H. 2009, *MNRAS*, 399, 2146
- Zacharias, N., Finch, C., Girard, T., et al. 2010, *AJ*, 139, 2184
- Zuckerman, B. & Song, I. 2004, *ARA&A*, 42, 685

**Table 1.** Confirmed members of Chamaeleon I and II with UCAC3 proper motions (excluding wrong measurements and interlopers)

2MASS J	Other names	UCAC3	$\mu_\alpha \cos \delta$ (mas/yr)	$\mu_\delta$ (mas/yr)	$V_r$ (km/s)	R (mag)	I (mag)	J (mag)	H (mag)	K (mag)	Notes
Chamaeleon I Cloud											
10463795-7736035	HD 93828	025-022840	-25.2 ± 0.9	-7.1 ± 1.0		13.298	12.637	7.844 ± 0.02	7.655 ± 0.06	7.477 ± 0.02	
10555973-7724399	T3A	026-024097	-5.7 ± 10.9	1.4 ± 7.0	13.4 ± 0.9	14.049	12.982	10.778 ± 1.27	9.832 ± 0.04	8.685 ± 0.02	(1)
10563044-7711393	SY Cha, T4	026-024109	-19.0 ± 4.7	7.4 ± 2.6	12.7 ± 0.1	13.339	12.421	9.969 ± 0.02	9.102 ± 0.02	8.631 ± 0.02	
10574219-7659356	Sz 4, T5	027-026396	-9.2 ± 7.6	0.0 ± 7.7	16.5 ± 1.3	14.754	13.329	10.433 ± 0.02	9.563 ± 0.02	9.246 ± 0.02	(1)
10581677-7717170	T6	026-024168	-22.5 ± 6.9	1.7 ± 2.7		12.182	10.893	9.253 ± 0.03	8.406 ± 0.04	7.758 ± 0.03	
10590108-7722407	SW Cha, T7	026-024197	-18.1 ± 1.8	4.6 ± 1.8	15.7 ± 1.2	13.496	12.891	10.135 ± 0.02	9.232 ± 0.02	8.616 ± 0.02	
10590699-7701404	CR Cha, T8	026-024202	-20.0 ± 1.3	4.7 ± 1.9	14.9 ± 0.8	14.231	13.295	8.462 ± 0.03	7.815 ± 0.04	7.31 ± 0.02	
11004022-7619280	T10	028-028320	-17.1 ± 8.2	-1.1 ± 5.5		16.027	14.561	11.859 ± 0.03	11.238 ± 0.02	10.871 ± 0.02	
11011875-7627025	CHXR 9C	028-028370	-14.1 ± 4.8	-7.5 ± 13.4		13.305	11.663	10.08 ± 0.03	9.307 ± 0.03	8.994 ± 0.02	
11022491-7733357	CS Cha, T11	025-023391	-20.2 ± 1.2	5.6 ± 2.7	14.7 ± 0.3	11.714	11.047	9.105 ± 0.03	8.452 ± 0.06	8.199 ± 0.03	(4)
11022610-7502407		030-032402	-17.9 ± 4.7	-4.5 ± 4.5		16.64	14.243	11.761 ± 0.03	11.115 ± 0.02	10.806 ± 0.02	
11023265-7729129	CHXR 71	026-024313	-19.3 ± 2.7	7.0 ± 5.9		16.357	14.764	11.268 ± 0.03	10.459 ± 0.02	10.129 ± 0.03	
11025504-7721508	T12	026-024325	-20.7 ± 3.2	8.5 ± 3.3		16.084	15.282	11.565 ± 0.03	10.858 ± 0.03	10.451 ± 0.02	
11035682-7721329	CHXR 12	026-024352	-19.3 ± 2.2	-2.5 ± 2.2		15.505	13.686	10.796 ± 0.02	9.994 ± 0.03	9.712 ± 0.02	
11040909-7627193	CT Cha, T14	028-028608	-18.9 ± 1.6	1.5 ± 1.6	15.1 ± 0.5	12.162	11.417	9.715 ± 0.02	8.944 ± 0.05	8.661 ± 0.02	
11045100-7625240	CHXR 14N	028-028660	-18.1 ± 1.9	4.3 ± 1.9		13.463	12.7	10.543 ± 0.03	9.831 ± 0.03	9.598 ± 0.02	
11045285-7625514	CHXR 14S	028-028661	-18.6 ± 2.5	1.1 ± 2.4		14.007	13.22	10.723 ± 0.02	9.981 ± 0.02	9.747 ± 0.02	
11050752-7812063		024-022792	-19.2 ± 13.2	-4.7 ± 5.3		16.535	14.615	11.776 ± 0.02	11.096 ± 0.02	10.816 ± 0.02	
11051467-7711290	Hn 4	026-024389	-23.7 ± 3.6	3.0 ± 3.5		16.425	15.139	10.944 ± 0.02	10.035 ± 0.03	9.608 ± 0.02	
11052472-7626209		028-028699	-21.1 ± 3.0	0.4 ± 3.1		15.539	14.009	11.474 ± 0.02	10.741 ± 0.02	10.522 ± 0.02	
11055261-7618255	T20	028-028735	-21.9 ± 2.0	0.7 ± 1.9		13.367	12.807	10.312 ± 0.02	9.593 ± 0.02	9.339 ± 0.02	
11061540-7721567	T21	026-024403	-19.2 ± 1.0	5.0 ± 1.6	17.0			7.597 ± 0.02	6.828 ± 0.05	6.419 ± 0.02	
11064346-7726343	T22	026-024409	-21.4 ± 3.5	-0.5 ± 3.7		16.252	14.776	10.813 ± 0.03	9.788 ± 0.03	9.392 ± 0.02	
11064510-7727023	CHXR 20	026-024411	-17.9 ± 2.4	5.6 ± 7.1		15.535	14.781	10.184 ± 0.02	9.197 ± 0.02	8.88 ± 0.02	
11065906-7718535	T23	026-024418	-18.3 ± 3.4	1.7 ± 4.6		16.199	15.368	11.204 ± 0.03	10.423 ± 0.02	10.003 ± 0.02	
11071148-7746394	CHXR 21	025-023408	-22.3 ± 3.9	3.0 ± 3.7		16.162	14.964	11.084 ± 0.03	10.083 ± 0.02	9.657 ± 0.02	
11071915-7603048	T25	028-028831	-22.1 ± 2.8	-2.0 ± 2.9		14.781	13.468	10.961 ± 0.02	10.092 ± 0.02	9.769 ± 0.02	
11072040-7729403	[LES2004]Chal 448, ISO 99	026-024421	-20.8 ± 2.8	2.8 ± 2.5		16.241	15.254	11.134 ± 0.02	10.547 ± 0.02	10.259 ± 0.02	
11072074-7738073	DI Cha, T26	025-023410	-15.8 ± 1.6	-5.1 ± 1.7	13.5 ± 0.6	14.455	13.013	7.819 ± 0.03	6.942 ± 0.04	6.217 ± 0.02	
11072825-7652118	VV Cha, T27	027-026870	-20.0 ± 1.9	-1.8 ± 1.9	15.4 ± 1.3	15.719	14.11	10.663 ± 0.03	9.905 ± 0.03	9.519 ± 0.02	
11074366-7739411	T28	025-023415	-19.8 ± 2.2	-0.3 ± 3.9		14.907	13.734	10.165 ± 0.02	8.975 ± 0.02	8.258 ± 0.03	
11075588-7727257	CHXR 28	026-024437	-28.8 ± 3.3	6.1 ± 3.4		15.038	13.725	9.215 ± 0.03	8.052 ± 0.03	7.691 ± 0.03	
11075792-7738449	T29	025-023419	-26.7 ± 5.7	13.7 ± 7.7		15.038	13.725	9.502 ± 0.03	7.919 ± 0.04	6.83 ± 0.02	(5)
11080148-7742288	VW Cha, T31	025-023420	-19.7 ± 1.3	-0.8 ± 3.4	15.1 ± 0.1	14.915	13.48	8.703 ± 0.03	7.637 ± 0.04	6.962 ± 0.03	
11080329-7739174	HD 97048, T32	025-023421	-17.8 ± 0.8	1.5 ± 0.8		14.726	13.679	7.267 ± 0.02	6.665 ± 0.05	5.941 ± 0.03	
11081509-7733531	T33A	025-023422	-2.1 ± 5.6	-4.4 ± 5.5		15.975	14.716	8.638 ± 0.03	7.729 ± 1.27	6.876 ± 1.27	(1)
11081648-7744371	T34	025-023423	-17.0 ± 3.1	-1.2 ± 4.1		15.822	17.073	11.198 ± 0.03	10.339 ± 0.03	10.024 ± 0.02	
11083905-7716042	T35	026-024448	-19.7 ± 3.0	1.2 ± 3.1		15.044	13.57	11.173 ± 0.03	9.904 ± 0.02	9.109 ± 0.02	
11084069-7636078	CHXR 33	027-026898	-17.3 ± 2.6	-0.8 ± 6.0		15.044	13.57	10.558 ± 0.02	9.658 ± 0.02	9.276 ± 0.02	
11085367-7521359	PU Car	030-033240	-5.5 ± 5.2	2.9 ± 5.1		16.279	14.393	10.98 ± 0.03	10.072 ± 0.03	9.556 ± 0.03	(1)
11085464-7702129	T38	026-024450	-18.4 ± 3.1	6.1 ± 2.7		15.032	14.147	11.208 ± 0.03	10.175 ± 0.02	9.457 ± 0.02	
11091769-7627578	CHXR 37, RXJ1109.4-7627	028-028916	-22.3 ± 1.8	-0.8 ± 9.9	13.1 ± 2.0	13.513	11.686	9.998 ± 0.02	9.044 ± 0.02	8.701 ± 0.02	(3)
11092379-7623207	VZ Cha, T40	028-028926	-20.9 ± 3.3	1.7 ± 2.6	14.7	15.058	13.993	10.44 ± 0.03	9.214 ± 0.02	8.242 ± 0.04	
11094006-7628391	CHXR 40	028-028940	-22.4 ± 6.8	4.0 ± 2.6		15.058	13.993	10.072 ± 0.02	9.23 ± 0.02	8.961 ± 0.02	
11095003-7636476	HD 97300, T41	027-026916	-17.7 ± 1.0	-2.7 ± 1.1		16.736	15.258	7.641 ± 0.03	7.347 ± 0.06	7.149 ± 0.02	(2)
11095407-7629253	T43	028-028953	-25.5 ± 6.4	2.5 ± 5.8		13.104	12.147	11.295 ± 0.03	10.003 ± 0.02	9.254 ± 0.02	
11095873-7737088	T45	025-023440	-20.9 ± 1.7	-0.6 ± 2.3		13.104	12.147	9.835 ± 0.03	8.768 ± 0.05	7.97 ± 0.02	

**Table 1.** (continued)

2MASS J	Other names	UCAC3	$\mu_\alpha \cos \delta$ (mas/yr)	$\mu_\delta$ (mas/yr)	$V_r$ (km/s)	R (mag)	I (mag)	J (mag)	H (mag)	K (mag)	Notes
11100469-7635452	T45a	027-026921	-16.3 ± 2.1	5.9 ± 2.1				10.565 ± 0.02	9.636 ± 0.02	9.24 ± 0.02	
11100704-7629376	T46	028-028961	-22.2 ± 1.8	-0.5 ± 1.8	12.9 ± 0.9			9.911 ± 0.02	8.964 ± 0.04	8.451 ± 0.03	
11101141-7635292	ISO 237	027-026922	-21.1 ± 5.6	5.1 ± 5.7				10.932 ± 0.03	9.438 ± 0.02	8.621 ± 0.02	
11103801-7732399	CHXR 47, WKK F34	025-023452	-20.3 ± 1.8	1.7 ± 1.8	14.0 ± 2.0	13.826	11.99	9.741 ± 0.03	8.687 ± 0.05	8.277 ± 0.03	(3)
11105333-7634319	T48	027-026930	-21.6 ± 2.6	-0.1 ± 2.8		15.064	13.723	11.259 ± 0.02	10.447 ± 0.02	10.038 ± 0.02	
11113474-7636211	CHXR 48	027-026948	-17.9 ± 9.9	-2.4 ± 2.2		15.741	14.367	10.864 ± 0.03	10.081 ± 0.02	9.802 ± 0.02	
11114632-7620092	CHX 18N	028-029063	-20.1 ± 1.4	0.8 ± 1.4	15.5	11.334	10.824	9.111 ± 0.03	8.286 ± 0.03	7.767 ± 0.03	(4)
11115400-7619311	CHXR 49NE	028-029070	-22.4 ± 1.8	-0.2 ± 1.8		13.893	12.16	10.203 ± 0.02	9.531 ± 0.03	9.233 ± 0.02	
11122441-7637064	CHX 20, T51, RXJ1112.7-7637	027-026990	-29.8 ± 4.3	4.7 ± 1.7	13.9 ± 0.4			9.275 ± 0.03	8.524 ± 0.06	7.999 ± 0.03	(3, 4)
11122772-7644223	CV Cha, T52	027-026995	-21.3 ± 1.1	1.9 ± 1.0	15.1 ± 0.3	16.96	12.953	8.285 ± 0.02	7.461 ± 0.04	6.845 ± 0.03	
11123092-7644241	CW Cha, T53	027-026996	-13.6 ± 3.2	4.2 ± 3.4				10.913 ± 0.03	9.854 ± 0.03	9.125 ± 0.02	(1, 2)
11124210-7658400	CHXR 54	027-027004	-22.4 ± 1.2	1.9 ± 2.5		12.693	11.816	10.409 ± 0.02	9.721 ± 0.02	9.499 ± 0.02	
11124268-7722230	T54	026-024473	-21.6 ± 1.0	4.8 ± 1.0				8.645 ± 0.03	8.042 ± 0.05	7.88 ± 0.03	
11124299-7637049	CHXR 55	027-027005	-21.6 ± 1.7	-1.9 ± 1.7				10.058 ± 0.03	9.4 ± 0.02	9.288 ± 0.02	
11132012-7701044	CHXR 57	026-024482	-20.9 ± 1.4	2.7 ± 2.0		15.836	14.439	10.884 ± 0.02	10.245 ± 0.03	10.013 ± 0.03	
11132112-7625558		028-029155	-27.2 ± 5.3	10.8 ± 2.7		10.519	8.432	5.436 ± 0.02	4.512 ± 0.08	4.128 ± 0.3	
11132446-7629227	Hn 18	028-029161	-24.6 ± 4.0	1.5 ± 3.4		16.094	14.367	11.855 ± 0.03	11.108 ± 0.02	10.797 ± 0.02	
11132737-7634165	CHXR 59	027-027042	-21.5 ± 1.8	-0.8 ± 1.8		13.993	12.487	10.606 ± 0.03	9.863 ± 0.03	9.634 ± 0.02	
11132970-7629012	CHXR 60	028-029171	-23.9 ± 3.5	-5.3 ± 3.4		16.029	14.136	11.569 ± 0.03	10.856 ± 0.02	10.577 ± 0.02	
11141565-7627364	CHXR 62	028-029208	-21.0 ± 3.5	3.4 ± 3.5		15.731	13.71	11.286 ± 0.02	10.465 ± 0.03	10.12 ± 0.02	
11145031-7733390	BYB 53	025-023572	-21.9 ± 1.6	2.5 ± 1.5		13.865	12.4	10.48 ± 0.03	9.75 ± 0.02	9.547 ± 0.02	
11155827-7729046		026-024615	-23.7 ± 4.0	9.0 ± 3.9		16.454	14.647	11.942 ± 0.03	11.311 ± 0.02	11.016 ± 0.02	
11173700-7704381	T56	026-024719	-21.8 ± 1.5	-1.7 ± 1.4		13.008	12.204	10.303 ± 0.02	9.575 ± 0.03	9.227 ± 0.02	
11175211-7629392		028-029527	-14.2 ± 5.5	3.6 ± 7.2		15.663	13.394	11.664 ± 0.04	11.151 ± 0.05	10.715 ± 0.04	(1)
11242980-7554237		029-033027	-9.4 ± 3.8	4.6 ± 4.2		15.837	13.418	10.931 ± 0.02	10.202 ± 0.02	9.884 ± 0.02	(1)
11253653-7700348		026-025416	-11.4 ± 2.0	5.0 ± 1.3		9.514	8.135	6.405 ± 0.02	5.543 ± 0.06	5.084 ± 0.02	(1)
Chamaeleon II Cloud											
12563364-7645453	Sz 46N	027-035004	-18.7 ± 5.4	23.0 ± 19.2	15.5 ± 1.2	14.128	12.943	11.253 ± 0.03	10.262 ± 0.03	9.758 ± 0.02	(1)
12565864-7647067	Sz 47	027-035025	-4.7 ± 2.8	-0.6 ± 2.8		13.711	13.342	12.84 ± 0.03	12.496 ± 0.02	12.247 ± 0.02	(1)
12571172-7640111	IRAS 12535-7623, CHIXR 2	027-035032	-26.3 ± 3.4	-12.4 ± 2.7	10.0 ± 1.5	13.383	11.791	10.037 ± 0.02	8.896 ± 0.02	8.395 ± 0.02	(1)
12592638-7747086	IRAS 12556-7731	025-031227	-7.0 ± 1.8	-4.1 ± 1.4		12.423	9.534	7.876 ± 0.02	6.862 ± 0.03	6.548 ± 0.02	(1)
13005323-7654151	Sz 49, Iso-Cha II 55, CHIXR 9	027-035312	-21.5 ± 6.5	-9.7 ± 21.8		16.74		11.823 ± 0.02	11.071 ± 0.02	10.633 ± 0.02	
13005532-7710222	Sz 50, Iso-Cha II 52, CHIXR 8	026-031723	-26.3 ± 4.0	-6.5 ± 3.7	13.0 ± 1.2	14.51	12.123	10.314 ± 0.02	9.325 ± 0.03	8.849 ± 0.02	
13005534-7708296	WFJ13005531-7708295	026-031722	-33.3 ± 10.1	-9.8 ± 8.6		15.22	13.17	11.175 ± 0.02	10.092 ± 0.03	9.691 ± 0.02	
13005622-7654021	RXJ1301.0-7654a	027-035316	-23.0 ± 2.6	-8.3 ± 2.5		11.174	10.201	9.031 ± 0.02	8.285 ± 0.04	8.095 ± 0.03	
13015891-7751218	Sz 51	025-031334	-20.7 ± 1.6	-11.9 ± 1.6		13.328	12.153	10.616 ± 0.02	9.849 ± 0.02	9.354 ± 0.02	
13030444-7707027	RXJ1303.1-7706	026-031811	-31.8 ± 2.0	-7.3 ± 1.8	12.4 ± 0.4	12.009	10.828	9.633 ± 0.02	8.9 ± 0.02	8.671 ± 0.02	
13042410-7650012	Hn 23	027-035636	5.1 ± 23.8	18.8 ± 21.6	15.2 ± 0.2	11.027	10.023	9.909 ± 0.03	9.109 ± 0.03	8.769 ± 0.03	(1)
13045571-7739495	Hn 24	025-031455	-25.6 ± 4.3	-7.2 ± 3.4		12.948	11.614	10.178 ± 0.02	9.302 ± 0.02	8.92 ± 0.02	
13052072-7739015	BF Cha, Sz 54	025-031467	-24.2 ± 1.7	-4.3 ± 1.8		14.473	12.969	9.052 ± 0.02	8.157 ± 0.04	7.597 ± 0.03	
13063053-7734001	Sz 55	025-031478	-14.1 ± 26.8	-4.9 ± 7.0		16.725	14.694	12.544 ± 0.02	11.556 ± 0.02	10.921 ± 0.02	
13065744-7723415	Sz 58, IRAS 13030-7707, [VCE2001]C61	026-032018	-27.9 ± 9.0	-8.0 ± 4.3	12.3 ± 4.3	14.348	13.68	10.841 ± 0.02	9.579 ± 0.03	8.755 ± 0.02	
13070922-7730304	Sz 59	025-031492	-19.2 ± 2.2	-12.8 ± 3.5	12.7 ± 2.7	12.535	12.069	10.517 ± 0.03	9.26 ± 0.03	8.381 ± 0.02	
13072241-7737225	Sz 60W	025-031495	-52.6 ± 20.4	-7.3 ± 4.5	13.2 ± 0.9	13.639	11.804	11.19 ± 0.06	10.224 ± 0.07	9.54 ± 0.04	(6)
13074851-7741214	Hn 26	025-031505	-16.3 ± 4.9	-3.8 ± 9.1		14.92	14.354	11.689 ± 0.02	10.62 ± 0.03	10.019 ± 0.02	
13080628-7755051	Sz 61	025-031510	-25.1 ± 2.1	-6.3 ± 2.0	12.0 ± 3.0	13.721	11.932	9.888 ± 0.02	8.761 ± 0.02	7.948 ± 0.02	
13095036-7757240	Sz 62	025-031562	-15.0 ± 5.4	-7.0 ± 2.3		13.736	12.248	10.522 ± 0.03	9.653 ± 0.03	9.119 ± 0.02	
13100415-7710447	Sz 63	026-032239	-25.3 ± 4.8	-3.0 ± 2.7		14.369	12.645	11.419 ± 0.03	10.707 ± 0.03	10.393 ± 0.02	

Table 1. (continued)

2MASS J	Other names	UCAC3	$\mu_{\alpha} \cos \delta$ (mas/yr)	$\mu_{\delta}$ (mas/yr)	$V_r$ (km/s)	R (mag)	I (mag)	J (mag)	H (mag)	K (mag)	Notes
13125238-7739182		025-031762	$-15.4 \pm 4.3$	$9.7 \pm 4.7$		15.191	12.824	$11.493 \pm 0.03$	$10.854 \pm 0.03$	$10.544 \pm 0.02$	(1)

Notes.

- (1) Dubious proper motion.
- (2) Discrepant proper motion form Hipparcos.
- (3) ROSAT source studied by Covino et al. (1997).
- (4) Spectroscopic binary.
- (5) Sometimes classified in the literature as a member of the  $\epsilon$  Cha cluster (see text for discussion).
- (6) Possible interloper from the  $\epsilon$  Cha cluster (see text for discussion).

**Table 2.** Kinematic members of the foreground  $\epsilon$  and  $\eta$  Chamaeleontis clusters (excluding wrong measurements and interlopers)

2MASS J	Other names	UCAC3	$\mu_\alpha \cos \delta$ (mas/yr)	$\mu_\delta$ (mas/yr)	Rv (km/s)	R (mag)	I (mag)	J (mag)	H (mag)	K (mag)	Notes
$\epsilon$ Chamaeleontis cluster											
10574936-6913599	CP-68 1388	042-083475	-35.8 $\pm$ 2.2	7.6 $\pm$ 2.3	15.9	13.941	12.741	8.484 $\pm$ 0.03	8.009 $\pm$ 0.05	7.792 $\pm$ 0.02	(1)
11080148-7742288	VW Cha, RXJ1108.1-7742	025-023420	-19.7 $\pm$ 1.3	-0. $\pm$ 3.4		14.915	13.48	8.703 $\pm$ 0.03	7.637 $\pm$ 0.04	6.962 $\pm$ 0.03	(2)
11183572-7935548	$\epsilon$ Cha 13	021-021275	-46.6 $\pm$ 4.5	4.4 $\pm$ 2.6		14.201	12.374	10.50 $\pm$ 0.03	9.891 $\pm$ 0.02	9.62 $\pm$ 0.02	(3)
11493184-7851011	DZ Cha	023-025652	-43.4 $\pm$ 2.9	-8. $\pm$ 1.8	12.2 $\pm$ 2.0	11.997	10.513	9.449 $\pm$ 0.02	8.721 $\pm$ 0.05	8.486 $\pm$ 0.02	(2)
11571348-7921313	T Cha, RXJ1157.2-7921	022-024424	-41.2 $\pm$ 3.2	-6. $\pm$ 1.4	20.0 $\pm$ 2.0	14.981	13.477	8.955 $\pm$ 0.03	7.86 $\pm$ 0.05	6.954 $\pm$ 0.02	(2)
11582681-7754450	GSC 9415-2676	025-027033	-38.5 $\pm$ 2.9	-7. $\pm$ 2.2	13.0 $\pm$ 2.0			10.34 $\pm$ 0.03	9.715 $\pm$ 0.03	9.436 $\pm$ 0.02	
11582816-7754294	DW Cha, RXJ1158.5-7754	025-027034	-40.4 $\pm$ 2.0	-2. $\pm$ 1.0	13.1 $\pm$ 2.0	14.084	12.967	8.219 $\pm$ 0.03	7.556 $\pm$ 0.04	7.404 $\pm$ 0.02	(2)
11594226-7601260	RXJ1159.7-7601	028-033151	-40.9 $\pm$ 2.1	-6. $\pm$ 1.8	13.1 $\pm$ 2.0	10.32	9.978	9.14 $\pm$ 0.03	8.469 $\pm$ 0.04	8.304 $\pm$ 0.03	(2)
12000829-7811395	HD 104237D	024-027122	-42.9 $\pm$ 7.1	27. $\pm$ 7.1				9.615 $\pm$ 0.06	8.744 $\pm$ 0.11	8.124 $\pm$ 0.21	(4)
12000931-7811424	HD 104237E	024-027125	7.3 $\pm$ 5.2	5.9 $\pm$ 5.2				9.104 $\pm$ 1.27	8.254 $\pm$ 1.27	7.488 $\pm$ 0.02	(4)
12013915-7859168	HD 104467, RXJ1201.7-7859	023-026618	-41.3 $\pm$ 1.0	-5. $\pm$ 1.0	10.0 $\pm$ 2.0			7.263 $\pm$ 0.03	6.967 $\pm$ 0.04	6.848 $\pm$ 0.02	(2)
12020369-7853012	GSC 9420-0948, RXJ1202.1-7853	023-026647	-41.0 $\pm$ 3.5	-4. $\pm$ 1.7	5.0 $\pm$ 2.0	14.944	13.629	9.215 $\pm$ 0.02	8.456 $\pm$ 0.04	8.307 $\pm$ 0.02	(2, 5)
12043615-7731345	GSC 9416-1029, RXJ1204.6-7731	025-027530	-38.8 $\pm$ 1.5	-2. $\pm$ 2.4	10.4 $\pm$ 2.0	12.879	11.306	9.765 $\pm$ 0.02	9.125 $\pm$ 0.02	8.881 $\pm$ 0.02	(2)
12074597-7816064	2MASS J12074597-7816064	024-027765	-53.4 $\pm$ 14.5	-15 $\pm$ 7.0		15.827	14.409	11.55 $\pm$ 0.02	10.98 $\pm$ 0.03	10.67 $\pm$ 0.02	
12113815-7110360	HD 105923, HIP 105923	038-075763	-37.9 $\pm$ 2.5	-8. $\pm$ 1.6	14.2	8.506	5.818	7.674 $\pm$ 0.02	7.308 $\pm$ 0.04	7.175 $\pm$ 0.03	
12194369-7403572	RXJ1219.7-7403, GSC 9239-1495	032-049103	-42.4 $\pm$ 4.2	-6. $\pm$ 1.9	13.1 $\pm$ 2.0	12.48	11.386	9.746 $\pm$ 0.03	9.048 $\pm$ 0.03	8.858 $\pm$ 0.02	(2)
12202177-7407393	GSC 9239-1572, RXJ1220.4-7407	032-049216	-40.6 $\pm$ 2.6	-5. $\pm$ 1.8	18.0 $\pm$ 2.0	11.836	10.565	9.26 $\pm$ 0.02	8.607 $\pm$ 0.03	8.367 $\pm$ 0.02	(2)
12392124-7502391	RXJ1239.4-7502, CD-74 712	030-043659	-40.7 $\pm$ 2.8	-13 $\pm$ 2.4	13.1 $\pm$ 2.0	9.537	8.346	8.434 $\pm$ 0.02	7.953 $\pm$ 0.03	7.777 $\pm$ 0.02	(2)
12582559-7028490	CD-69 1055	040-110662	-40.9 $\pm$ 2.6	-17 $\pm$ 1.1	12.8	9.558	7.938	8.184 $\pm$ 0.03	7.702 $\pm$ 0.06	7.545 $\pm$ 0.03	
13021351-7637577	CM Cha, IRAS 12584-7621	027-035419	-43.3 $\pm$ 10.6	7.5 $\pm$ 9.1		12.04	10.936	10.02 $\pm$ 0.02	9.165 $\pm$ 0.03	8.515 $\pm$ 0.02	(3)
13220753-6938121	MP Mus	041-134775	-40.4 $\pm$ 1.0	-20 $\pm$ 1.6	11.6 $\pm$ 0.2			8.277 $\pm$ 0.03	7.641 $\pm$ 0.02	7.293 $\pm$ 0.02	
$\eta$ Chamaeleontis cluster											
08365623-7856454	EG Cha, RECX 1	023-014604	-27.1 $\pm$ 1.0	25.3 $\pm$ 1.0	18.0 $\pm$ 2.0	9.359	8.525	8.155 $\pm$ 0.02	7.498 $\pm$ 0.05	7.338 $\pm$ 0.02	(2)
08413703-7903304	EH Cha, RECX 3	022-014105	-29.5 $\pm$ 2.2	33.6 $\pm$ 2.2		15.595	13.998	10.349 $\pm$ 0.02	9.647 $\pm$ 0.02	9.415 $\pm$ 0.02	
08414471-7902531	HD 75505	022-014112	-30.3 $\pm$ 1.4	25.0 $\pm$ 1.8		7.148	6.776	7.059 $\pm$ 0.03	6.987 $\pm$ 0.04	6.928 $\pm$ 0.02	
08422372-7904030	EI Cha, RECX 4	022-014146	-27.9 $\pm$ 10.7	17.9 $\pm$ 2.4		14.993	13.508	9.535 $\pm$ 0.02	8.779 $\pm$ 0.06	8.615 $\pm$ 0.02	
08422710-7857479	EK Cha, RECX 5	023-014912	-30.8 $\pm$ 2.7	35.1 $\pm$ 4.7		14.229	12.114	10.777 $\pm$ 0.02	10.099 $\pm$ 0.02	9.855 $\pm$ 0.02	
08423879-7854427	EL Cha, RECX 6	023-014921	-35.7 $\pm$ 2.3	25.0 $\pm$ 2.4		13.023	11.39	10.232 $\pm$ 0.03	9.584 $\pm$ 0.02	9.29 $\pm$ 0.02	
08430723-7904524	EM Cha, RECX 7	022-014185	-29.7 $\pm$ 1.9	25.3 $\pm$ 3.1	4.3 $\pm$ 2.0			8.42 $\pm$ 0.02	7.758 $\pm$ 0.03	7.635 $\pm$ 0.03	(2, 5)
08431857-7905181	ET Cha, RECX 15	022-014197	-14.2 $\pm$ 20.9	36.0 $\pm$ 28.9		15.144	13.742	10.505 $\pm$ 0.03	9.834 $\pm$ 0.02	9.431 $\pm$ 0.02	
08441637-7859080	EN Cha, RECX 9	023-015007	-29.5 $\pm$ 2.4	27.5 $\pm$ 2.7		13.795	11.695	10.26 $\pm$ 0.03	9.668 $\pm$ 0.03	9.335 $\pm$ 0.02	
08443188-7846311	EO Cha, RECX 10	023-015019	-31.6 $\pm$ 2.0	25.2 $\pm$ 1.9	15.0 $\pm$ 2.0	11.659	10.287	9.653 $\pm$ 0.02	8.919 $\pm$ 0.06	8.732 $\pm$ 0.02	(2)
08470165-7859345	EP Cha, RECX 11	023-015143	-30.7 $\pm$ 1.2	26.0 $\pm$ 1.2		10.311	9.438	8.729 $\pm$ 0.02	8.025 $\pm$ 0.06	7.655 $\pm$ 0.04	
08475676-7854532	EQ Cha, RECX 12	023-015181	-32.1 $\pm$ 1.8	26.8 $\pm$ 1.8	18.0 $\pm$ 2.0	12.076	10.534	9.323 $\pm$ 0.02	8.683 $\pm$ 0.08	8.41 $\pm$ 0.03	(2)

**Notes.**

- (1) Possible interloper (see text for discussion).
- (2) ROSAT source studied by Covino et al. (1997).
- (3) Classified in the literature as a Chamaeleon I or II member.
- (4) Dubious proper motion.
- (5) Discrepant radial velocity respect the mean group value.

**Table 3.** Background objects.

2MASS J	Other names	UCAC3	$\mu_\alpha \cos \delta$ (mas/yr)	$\mu_\delta$ (mas/yr)
10452780-7715335		026-023750	$1.2 \pm 2.2$	$7.2 \pm 4.6$
11001473-7757103		025-023372	$-10.7 \pm 4.5$	$15.1 \pm 2.7$
11014949-7412268		032-038265	$-4.8 \pm 3.9$	$1.7 \pm 3.2$
11035902-7743349	ISO 35	025-023396	$1.5 \pm 3.8$	$-4.4 \pm 2.9$
11045890-7656550		027-026781	$-6.5 \pm 4.0$	$16.1 \pm 16.8$
11050937-7706578		026-024388	$-8.6 \pm 1.6$	$6.0 \pm 1.7$
11051798-7706565		026-024390	$5.3 \pm 3.0$	$8.3 \pm 2.1$
11052489-7620373		028-028700	$-1.4 \pm 3.4$	$0.3 \pm 1.7$
11052850-7639489		027-026798	$-11.3 \pm 2.3$	$2.3 \pm 3.1$
11053587-7638034		027-026805	$-8.9 \pm 3.8$	$-2.0 \pm 1.8$
11054972-7640462		027-026814	$-0.1 \pm 1.8$	$4.9 \pm 1.8$
11055683-7656438		027-026817	$-15.1 \pm 1.9$	$11.0 \pm 1.9$
11063479-7645404		027-026840	$-43.9 \pm 2.1$	$15.5 \pm 3.5$
11063841-7612032		028-028775	$-1.9 \pm 2.6$	$4.1 \pm 2.6$
11064235-7632450		027-026847	$-4.0 \pm 3.1$	$2.2 \pm 3.2$
11064274-7636124		027-026848	$-5.9 \pm 1.8$	$9.8 \pm 2.4$
11064586-7625317		028-028787	$-0.8 \pm 1.8$	$2.3 \pm 3.4$
11065986-7651181		027-026858	$-4.4 \pm 1.6$	$1.5 \pm 1.6$
11070350-7631443		027-026861	$-1.0 \pm 2.9$	$7.4 \pm 2.9$
11070380-7635440		027-026862	$-72.5 \pm 1.4$	$30.2 \pm 1.3$
11073280-7748594	ISO 104	025-023413	$1.5 \pm 2.4$	$1.9 \pm 2.3$
11074763-7711156		026-024434	$-7.1 \pm 1.6$	$2.1 \pm 1.6$
11075699-7741558	ISO 118	025-023418	$-21.2 \pm 6.7$	$-1.3 \pm 5.3$
11081069-7637424		027-026887	$-0.3 \pm 2.2$	$-3.1 \pm 2.2$
11081916-7656525	ISO 139	027-026889	$-13.1 \pm 2.5$	$3.0 \pm 3.4$
11083897-7614457		028-028890	$-3.9 \pm 1.9$	$2.4 \pm 1.9$
11085527-7704502	ISO 166	026-024451	$-13.4 \pm 1.6$	$6.3 \pm 1.6$
11085813-7646392	ISO 170	027-026908	$-34.0 \pm 2.5$	$12.3 \pm 2.5$
11090332-7700495	ISO 172	026-024453	$12.7 \pm 7.4$	$9.6 \pm 7.4$
11090367-7707456	ISO 175	026-024454	$5.3 \pm 1.9$	$0.6 \pm 1.9$
11090766-7618144		028-028907	$-4.3 \pm 1.4$	$6.2 \pm 1.4$
11091379-7637531	ISO 183	027-026913	$4.3 \pm 2.0$	$10.9 \pm 2.1$
11092068-7713591	ISO 188	026-024457	$-5.3 \pm 2.7$	$-5.6 \pm 2.8$
11092482-7642073	ISO 191	027-026915	$-5.5 \pm 3.5$	$1.2 \pm 3.5$
11095119-7658568	ISO 213	027-026917	$-82.0 \pm 1.0$	$17.6 \pm 1.1$
11095465-7625333		028-028954	$1.8 \pm 3.0$	$1.1 \pm 3.1$
11095822-7659147	[LM04]ChaI 616, ISO 229	027-026919	$-3.2 \pm 2.6$	$4.8 \pm 2.6$
11102819-7626164	ISO 242	028-028979	$-22.1 \pm 1.3$	$5.0 \pm 1.3$
11102990-7736064	ISO 243	025-023448	$-3.0 \pm 4.1$	$7.9 \pm 4.4$
11103067-7637186	ISO 245	027-026923	$-6.3 \pm 3.3$	$0.5 \pm 2.8$
11105038-7631440	ISO 255	027-026928	$-6.9 \pm 5.9$	$8.4 \pm 2.0$
11105215-7709286	ISO 257	026-024459	$-1.4 \pm 1.8$	$-7.6 \pm 1.8$
11110383-7706261	ISO 263	026-024460	$6.2 \pm 3.2$	$1.7 \pm 4.4$
11110670-7717594	ISO 264	026-024461	$6.3 \pm 2.2$	$10.7 \pm 2.2$
11110714-7722056	ISO 265	026-024462	$-9.3 \pm 4.8$	$-0.3 \pm 2.9$
11111062-7657205	ISO 267	027-026938	$-4.9 \pm 2.1$	$8.5 \pm 2.1$
11111680-7628573		028-029023	$7.3 \pm 15.6$	$4.8 \pm 21.1$
11131188-7647392		027-027030	$-6.7 \pm 2.5$	$-3.3 \pm 2.4$
11173079-7627078		028-029481	$-2.6 \pm 1.2$	$5.8 \pm 1.0$
11195060-7628492		028-029694	$-7.5 \pm 6.9$	$0.1 \pm 4.3$
11213026-7805240		024-023578	$-2.8 \pm 2.5$	$2.6 \pm 4.5$
11225703-7649560		027-027766	$-8.7 \pm 1.1$	$6.4 \pm 2.6$



**Table 7.** Kinematic properties of ROSAT stars not included in our initial member lists

RXJ	2MASS J	Other names	UCAC3	$\mu_\alpha \cos \delta$ (mas/yr)	$\mu_\delta$ (mas/yr)	$V_r$ (km/s)	Evolutionary status <sup>a</sup>	Group <sup>b</sup>
1129.2-7546	11291261-7546263		029-033458	-24.5±1.5	-2.1±1.5	11.4±2.0	PMS	Cha I
1158.5-7913	11583429-7913175		022-024487	-18.3±3.8	-3.1±1.9	13.1±2.0	PMS	Cha I?
1123.2-7924	11225562-7924438	$\epsilon$ Cha 14	022-022912	-29.8±2.1	-19.0±1.7	10.0±2.0	PMS	$\epsilon$ Cha?
1150.4-7704	11502829-7704380	$\epsilon$ Cha 19	026-027460	-40.3±1.2	-8.3±1.5		PMS	$\epsilon$ Cha
1216.8-7753	12164593-7753333		025-028496	-37.5±1.6	-8.0±1.6	14.0±2.0	PMS	$\epsilon$ Cha
0850.1-7554	08500540-7554380		029-020107	-15.9±1.1	33.0±0.9	15.5±2.0	PMS	$\eta$ Cha
0902.9-7759			025-017479	-34.6±1.7	22.4±1.7	11.0±2.0	PMS	$\eta$ Cha
0915.5-7608	09152912-7608471		028-021037	-29.3±2.0	18.9±1.4	21.0±2.0	PMS	$\eta$ Cha
0928.5-7815	09282116-7815352	HD 82879	024-017885	-25.4±1.0	18.0±1.5	16.8±2.0	?	$\eta$ Cha
0935.0-7804	09345604-7804193		024-018258	-28.6±1.3	19.2±1.3	14.0±2.0	PMS	$\eta$ Cha
0951.9-7901	09515069-7901377	HD 86356	022-017379	-26.4±0.8	38.5±0.8	12.2±2.0	PMS	$\eta$ Cha
1001.1-7913	10010873-7913074		022-017956	-25.0±1.5	38.7±2.3	12.2±2.0	PMS	$\eta$ Cha
1140.3-8321	11401658-8321003		014-014885	-41.7±1.1	27.7±1.1	10.5±2.0	?	$\eta$ Cha
1017.9-7431	10175369-7431172		031-030277	-6.5±2.1	6.6±1.3	104.0±2.0	ZAMS	Field
1035.8-7859	10354856-7858583		023-020966	-65.9±5.5	6.2±3.0	70.8±2.0	ZAMS	Field
1044.6-7849	10443523-7849244		023-021597	-87.6±2.3	25.9±4.3	-8.4±2.0	ZAMS	Field
0842.4-8345	08422284-8345248		013-008994	-49.5±1.3	91.2±1.2	-8.0±2.0	?	Field
0849.2-7735	08491110-7735585		025-016705	-11.5±1.2	16.3±1.1	-3.4±2.0	?	Field
0853.1-8244	08530528-8243597		015-010451	0.5±0.9	-14.4±1.1	7.7±2.0	?	Field
0936.3-7820	09361783-7820417	HD 84075	024-018347	-73.4±0.8	50.1±0.8	3.2±2.0	?	Field
0946.9-8011	09465051-8011352		020-015930	-16.8±1.9	-3.9±3.9	5.4±2.0	?	Field
0952.7-7933a	09531375-7933285	HD 86588	021-016442	-13.5±0.9	2.0±0.9	2.0±2.0	?	Field
1007.7-8504	10072939-8504329	DR Oct, HD 89499	010-008728	-566.0±	395.0±	-67.1±2.0	?	Field
1009.6-8105	10093502-8105509		018-015349	-15.4±4.5	12.0±3.8	8.8±2.0	?	Field
1014.2-7636	10140807-7636327		027-023785	-47.2±1.7	30.6±3.6	8.0±2.0	?	Field
1014.4-8138	10142048-8138423		017-014665	-36.5±1.3	17.4±2.0	6.6±2.0	?	Field
1048.9-7655	10485467-7655450		027-025899	-95.6±1.4	45.7±2.1	-19.9±2.0	?	Field
1207.9-7555	12075118-7555159		029-037031	-156.7±2.6	-1.5±2.0	-3.4±2.0	?	Field
1209.8-7344	12094282-7344414		033-053854	-9.3±2.3	-3.2±1.3	1.0±2.0	?	Field
1217.4-8035	12172694-8035069	HD 106772	019-022395	-0.4±1.5	-10.4±1.4	-13.0±2.0	?	Field
1220.6-7539	12203437-7539286		029-038424	-111.2±1.5	4.0±1.0	6.0±2.0	?	Field
1223.5-7740	12232906-7740514	HD 107722	025-029020	-66.8±1.2	11.9±1.4	10.4±2.0	?	Field
1225.3-7857	12251340-7857347		023-028311	-27.0±1.0	-16.4±1.6	-6.7±2.0	?	Field
1233.5-7523	12332981-7523112	HD 109138	030-042831	-94.4±1.1	16.3±1.0	14.0±2.0	?	Field
1307.3-7602	13072289-7602360		028-039286	-19.1±1.5	1.7±1.2	-62.8±2.0	?	Field
1349.2-7549E	13491293-7549475		029-049787	-61.7±1.0	-32.3±1.7	1.0±2.0	?	Field

**Notes.**<sup>a</sup> Covino et al. (1997)<sup>b</sup> This work (a question mark if dubious, see text)

**Table 8.** UCAC3 proper motions for candidate members of the Chamaeleon dark clouds from the literature

2MASS J	Other names	UCAC3	$\mu_{\alpha} \cos \delta$ (mas/yr)	$\mu_{\delta}$ (mas/yr)	$R_{phot}$ mag	$I_{phot}$ mag	J mag	H mag	K mag	Ref. <sup>(a)</sup>	Notes <sup>(b)</sup>
11094646-7628575	C1-14	028-028944	$-27.4 \pm 2.0$	$10.2 \pm 1.0$	13.977	13.111	$8.432 \pm 0.04$	$8.035 \pm 0.06$	$7.854 \pm 0.02$	1	C
Chamaeleon I Cloud											
12482571-7706366	IRAS 12448-7650	026-031454	$-5.4 \pm 1.8$	$4.2 \pm 1.7$	13.507	9.872	$6.789 \pm 0.02$	$5.674 \pm 0.02$	$5.177 \pm 0.02$	2	R
12540028-7624251	[VCE2001]C18	028-038152	$-1.4 \pm 4.4$	$0.6 \pm 5.9$	14.894	11.308	$8.194 \pm 0.03$	$7.139 \pm 0.05$	$6.606 \pm 0.02$	3	R
12551447-7622005	[VCE2001]C29	028-038240	$-6.6 \pm 10.2$	$7.1 \pm 4.6$	15.36	12.238	$10.053 \pm 0.02$	$9.063 \pm 0.02$	$8.673 \pm 0.02$	3	R
13024772-7702399	IRAS 12589-7646, Iso-Cha II 89	026-031795	$-21.2 \pm 3.9$	$7.9 \pm 9.3$	13.179	9.554	$7.196 \pm 0.02$	$6.199 \pm 0.03$	$5.716 \pm 0.02$	2	R
13024919-7705448	[VCE2001]X3	026-031797	$-24.6 \pm 5.3$	$5.9 \pm 6.0$	15.889	15.483	$14.315 \pm 0.03$	$13.839 \pm 0.04$	$13.597 \pm 0.04$	3	R
13030903-7700328	[VCE2001]X4	026-031820	$-11.3 \pm 5.8$	$-13.7 \pm 4.0$	13.597	12.954	$12.465 \pm 0.02$	$12.1 \pm 0.03$	$11.991 \pm 0.03$	3	R
13074107-7805434	[VCE2001]C64	024-032467	$-12.9 \pm 5.4$	$0.8 \pm 14.7$	15.605	13.072	$10.458 \pm 0.02$	$9.118 \pm 0.02$	$8.641 \pm 0.02$	3	R
Chamaeleon II Cloud											

**Notes.**<sup>a</sup> References: 1) Luhman et al. (2004); Spezzi et al. (2008); Vuong et al. (2001)<sup>b</sup> Notes: C=confirmed as probable kinematical member; R=rejected candidate (proper motion not consistent with membership).

**Table 9.** Space velocities for members and candidate members of the Chamaeleon associations.

Name	$U$ (km/s)	$V$ (km/s)	$W$ (km/s)	$U_{LSR}$ (km/s)	$V_{LSR}$ (km/s)	$W_{LSR}$ (km/s)	Notes
Chamaeleon I cloud							
T3A	$-1.8 \pm 7.3$	$-13.2 \pm 3.4$	$-4.6 \pm 5.8$	-10.3	0.2	1.9	
SY Cha	$8.5 \pm 3.3$	$-17.5 \pm 1.4$	$-4.8 \pm 2.5$	-0.0	-4.1	1.7	
Sz 4	$-1.1 \pm 5.3$	$-16.3 \pm 3.2$	$-7.4 \pm 5.6$	-9.6	-2.9	-0.9	
TW Cha	$5.9 \pm 1.7$	$-19.0 \pm 1.3$	$-7.0 \pm 1.6$	-2.6	-5.7	-0.5	
CR Cha	$7.6 \pm 1.5$	$-18.8 \pm 1.0$	$-7.3 \pm 1.6$	-0.9	-5.5	-0.8	
CS Cha	$7.9 \pm 1.5$	$-19.1 \pm 1.0$	$-6.6 \pm 2.1$	-0.6	-5.7	-0.1	
CT Cha	$6.1 \pm 1.6$	$-18.0 \pm 0.8$	$-8.6 \pm 1.3$	-2.4	-4.6	-2.2	
T21	$14.3 \pm 3.3$	$-20.9 \pm 1.4$	$-8.8 \pm 2.0$	5.8	-7.5	-2.3	
DI Cha	$3.4 \pm 1.5$	$-13.8 \pm 1.0$	$-11.8 \pm 1.3$	-5.1	-0.4	-5.3	
VV Cha	$6.0 \pm 1.9$	$-17.6 \pm 1.4$	$-11.2 \pm 1.5$	-2.5	-4.2	-4.7	
VW Cha	$6.1 \pm 1.6$	$-17.5 \pm 1.2$	$-10.5 \pm 2.4$	-2.4	-4.1	-4.9	
CHXR 37	$8.7 \pm 2.8$	$-16.6 \pm 3.4$	$-10.4 \pm 6.7$	0.2	-3.2	-3.9	
VZ Cha	$6.1 \pm 1.7$	$-17.5 \pm 1.2$	$-10.5 \pm 2.4$	-2.4	-4.1	-4.0	
T46	$8.8 \pm 1.9$	$-16.5 \pm 1.2$	$-10.0 \pm 1.5$	0.3	-3.1	-3.6	
CHXR 47	$7.4 \pm 1.9$	$-17.5 \pm 1.9$	$-8.5 \pm 1.6$	-1.1	-4.2	-2.0	
CHX 18N	$8.5 \pm 3.3$	$-17.5 \pm 1.4$	$-4.8 \pm 2.5$	-0.0	-4.1	1.7	
CHX 20	$14.3 \pm 3.3$	$-20.9 \pm 1.4$	$-8.8 \pm 2.0$	5.8	-7.5	-2.3	
CV Cha	$6.1 \pm 5.0$	$-18.3 \pm 1.8$	$-8.1 \pm 2.9$	-2.4	-4.9	-1.6	(1)
RXJ1129.2-7546	$10.8 \pm 2.0$	$-16.2 \pm 2.0$	$-10.0 \pm 1.3$	2.3	-2.8	-3.5	
RXJ1158.5-7913	$5.7 \pm 2.8$	$-16.1 \pm 2.3$	$-8.8 \pm 1.7$	-2.8	-2.8	-2.3	(2)
Mean values ( $\sigma$ )	7.0 (3.8)	-17.4 (1.9)	-8.4 (2.1)	-1.5 (3.8)	-4.1 (1.9)	-2.0 (2.1)	
Chamaeleon II cloud							
Sz 46N	$2.0 \pm 5.5$	$-25.0 \pm 2.9$	$15.4 \pm 15.9$	-6.5	-11.6	21.9	
IRAS 12535-7623	$14.7 \pm 3.3$	$-18.4 \pm 2.4$	$-12.0 \pm 2.4$	6.2	-5.1	-5.6	
Sz 50	$12.4 \pm 3.5$	$-21.9 \pm 2.5$	$-7.7 \pm 3.1$	3.9	-8.5	-1.2	
RXJ1303.1-7706	$16.6 \pm 2.7$	$-24.0 \pm 1.8$	$-7.8 \pm 1.5$	8.1	-10.6	-1.3	
Hn 23	$-14.5 \pm 16.8$	$-12.6 \pm 11.4$	$11.5 \pm 18.1$	-23.0	0.8	18.0	
Sz 58	$14.0 \pm 6.9$	$-22.1 \pm 5.7$	$-8.2 \pm 3.8$	5.5	-8.7	-1.7	
Sz 59	$8.5 \pm 2.7$	$-17.5 \pm 2.6$	$-12.7 \pm 3.0$	0.0	-4.2	-6	
Sz 60W	$30.5 \pm 14.4$	$-34.8 \pm 10.1$	$-6.6 \pm 4.8$	22.0	-21.4	-0.1	
Sz 61	$12.0 \pm 2.9$	$-20.7 \pm 2.9$	$-6.9 \pm 1.8$	3.5	-7.4	-0.4	
Mean values ( $\sigma$ )	10.7 (11.4)	-21.9 (5.8)	-3.9 (9.5)	2.2 (11.4)	-8.5 (5.8)	2.6 (9.5)	
$\epsilon$ Chamaeleontis cluster							
CM Cha	$9.6 \pm 4.8$	$-26.3 \pm 3.3$	$1.0 \pm 4.8$	1.1	-13.0	7.5	(3)
T Cha	$18.1 \pm 13.6$	$-28.9 \pm 7.5$	$-16.9 \pm 3.6$	9.6	-15.5	-10.4	(1, 4)
DW Cha	$12.2 \pm 1.5$	$-19.9 \pm 1.9$	$-9.1 \pm 0.7$	3.7	-6.5	-2.6	
RXJ1159.7-7601	$12.3 \pm 1.6$	$-19.7 \pm 1.9$	$-10.3 \pm 1.0$	3.8	-6.3	-3.9	
HD 104467	$14.0 \pm 1.4$	$-17.1 \pm 1.8$	$-9.5 \pm 0.6$	5.5	-3.7	-3.0	
RXJ1219.7-7403	$12.7 \pm 2.3$	$-21.1 \pm 2.1$	$-8.5 \pm 1.1$	4.2	-7.7	-2.0	
RXJ1239.4-7502	$11.9 \pm 1.8$	$-20.6 \pm 1.9$	$-10.8 \pm 1.3$	3.4	-7.2	-4.3	
DZ Cha	$13.8 \pm 1.9$	$-18.3 \pm 1.9$	$-12.8 \pm 1.1$	5.3	-4.9	-6.3	
GSC 9420-0948	$16.3 \pm 2.0$	$-13.1 \pm 2.0$	$-7.5 \pm 1.1$	7.8	0.3	-1.0	
GSC 9416-1029	$12.7 \pm 1.4$	$-17.6 \pm 1.8$	$-7.5 \pm 1.2$	4.2	-4.2	-1.0	
GSC 9239-1572	$9.4 \pm 1.8$	$-24.9 \pm 1.9$	$-8.9 \pm 1.0$	0.9	-11.5	-2.4	
CP-68 1388	$11.3 \pm 1.3$	$-21.2 \pm 0.6$	$-6.8 \pm 1.2$	2.8	-7.8	-0.3	
HD 105923	$10.1 \pm 1.4$	$-20.6 \pm 0.8$	$-9.8 \pm 0.9$	1.6	-7.2	-3.3	
GSC 9415-2676	$11.2 \pm 1.8$	$-18.5 \pm 1.9$	$-11.3 \pm 1.2$	2.7	-5.1	-4.8	
CD-69 1055	$11.7 \pm 1.4$	$-21.7 \pm 0.9$	$-10.0 \pm 0.7$	3.2	-8.3	-3.5	
MP Mus	$12.0 \pm 0.9$	$-21.6 \pm 0.6$	$-9.3 \pm 0.9$	3.5	-8.2	-2.8	
RXJ1123.2-7924	$7.3 \pm 1.5$	$-9.9 \pm 1.9$	$-17.2 \pm 1.0$	-1.2	3.5	-10.7	(5)
RXJ1216.8-7753	$10.2 \pm 1.5$	$-19.8 \pm 1.8$	$-10.3 \pm 0.8$	1.7	-6.4	-3.8	
Mean values ( $\sigma$ )	12.1 (2.4)	-20.0 (4.1)	-9.7 (3.7)	3.6 (2.4)	-6.6 (4.1)	-3.2 (3.7)	
$\eta$ Chamaeleontis cluster							
EG Cha	$9.5 \pm 0.9$	$-20.0 \pm 1.4$	$-11.1 \pm 1.6$	1.0	-6.7	-4.6	
EM Cha	$15.0 \pm 1.2$	$-8.4 \pm 1.7$	$-6.6 \pm 1.8$	6.5	4.9	-0.1	
EO Cha	$11.8 \pm 1.2$	$-17.6 \pm 1.5$	$-11.0 \pm 1.7$	3.3	-4.2	-4.6	
EQ Cha	$11.4 \pm 1.1$	$-20.7 \pm 1.5$	$-11.7 \pm 1.7$	2.9	-7.3	-5.2	
RXJ0850.1-7554	$10.3 \pm 0.8$	$-20.2 \pm 1.4$	$-2.7 \pm 1.6$	1.8	-6.9	3.8	
RXJ0902.9-7759	$13.4 \pm 1.1$	$-14.2 \pm 1.5$	$-9.9 \pm 1.6$	4.9	-0.8	-3.4	
RXJ0915.5-7608	$7.7 \pm 1.2$	$-22.8 \pm 1.5$	$-11.0 \pm 1.5$	-0.8	-9.4	-4.5	
HD 82879	$7.0 \pm 1.0$	$-19.2 \pm 1.5$	$-8.3 \pm 1.4$	-1.5	-5.8	-1.8	
RXJ0935.0-7804	$9.4 \pm 1.0$	$-17.4 \pm 1.6$	$-7.5 \pm 1.4$	0.9	-4.0	-1.1	
HD 86356	$13.4 \pm 0.9$	$-20.7 \pm 1.6$	$0.9 \pm 1.4$	4.9	-7.3	7.4	
RXJ1001.1-7913	$12.5 \pm 1.1$	$-20.9 \pm 1.8$	$2.0 \pm 1.6$	4.0	-7.6	8.6	
RXJ1140.3-8321	$12.7 \pm 1.2$	$-21.7 \pm 1.8$	$2.5 \pm 1.2$	4.2	-8.3	8.9	
Mean values ( $\sigma$ )	11.2 (2.3)	-18.7 (3.8)	-6.2 (5.2)	2.7 (2.3)	-5.3 (3.8)	0.3 (5.2)	

**Notes.**

(1) The distance inferred from the Hipparcos parallax (Table 5) was used in the calculation.

(2) Assuming the distance to  $\epsilon$  Cha for this star, the following space velocities are obtained ( $U, V, W$ ) = ( $2.0 \pm 2.0, -14.5 \pm 2.0, -7.2 \pm 1.2$ ) km/s(3) If the distance to Cha II is assumed for this object, the resulting space velocities are ( $U, V, W$ ) = ( $20.6 \pm 8.0, -34.5 \pm 5.5, 3.9 \pm 7.7$ ) km/s(4) With a parallax  $\pi = 15.06 \pm 3.31$ , we obtain for this star ( $U, V, W$ ) = ( $1.5 \pm 7.0, -21.5 \pm 8.1, -10.2 \pm 3.7$ ) km/s(5) Assuming the distance to Cha II for this star, we obtain ( $U, V, W$ ) = ( $14.5 \pm 3.2, -10.8 \pm 2.4, -25.7 \pm 1.6$ ) km/s

Table 10: Physical parameters for kinematic members of the Chamaeleon clouds<sup>a</sup>

2MASS J	Class	$T_{eff}$ K	$L_{bol}$ Lsun
Chamaeleon I Cloud			
11022491-7733357	II	4205	1.2
11023265-7729129	II	3415	0.17
11025504-7721508	II	3198	0.081
11035682-7721329	III	3342	0.21
11040909-7627193	II	4350	0.95
11045100-7625240	III	3955	0.35
11045285-7625514	III	3596	0.26
11051467-7711290	III	3379	0.31
11055261-7618255	III	3632	0.35
11061540-7721567	III	5770	16.0
11064346-7726343	III	3415	0.42
11064510-7727023	II	4205	1.1
11065906-7718535	II	3234	0.11
11071148-7746394	III	3415	0.34
11071915-7603048	III	3488	0.24
11072074-7738073	II	5860	12.0
11074366-7739411	II	3850	1.4
11075588-7727257	III	4205	4.0
11075792-7738449	Flat	4205	2.4
11080148-7742288	II	3955	3.0
11080329-7739174	II	10010	70.0
11081648-7744371	III	3306	0.15
11083905-7716042	II	3955	0.53
11084069-7636078	III	3488	0.74
11085464-7702129	II	3778	0.34
11091769-7627578	III	4060	1.1
11092379-7623207	II	4205	0.53
11094006-7628391	III	3669	0.68
11095407-7629253	II	3560	0.48
11095873-7737088	II	3669	0.84
11100469-7635452	II	3705	0.43
11100704-7629376	II	3850	1.4
11101141-7635292	II	4278	1.2
11103801-7732399	II	4730	2.6
11105333-7634319	II	3306	0.13
11113474-7636211	III	3488	0.21
11114632-7620092	II	4205	1.3
11115400-7619311	III	3488	0.36
11122441-7637064	II	4660	1.0
11122772-7644223	II	5410	5.0
11124268-7722230	II	5520	4.2
11124299-7637049	III	4470	0.61
11132446-7629227	II	3342	0.073
11132737-7634165	III	3451	0.24
11132970-7629012	III	3234	0.089
11141565-7627364	III	3306	0.15
11145031-7733390	III	3451	0.24
Chamaeleon II Cloud			
12571172-7640111	II	3850	1.38
13005323-7654151	II	3777	0.20
13005532-7710222	II	3415	1.15
13005534-7708296	III	3687	0.355
13015891-7751218	II	3955	0.44
13030444-7707027	III	3850	1.26
13045571-7739495	II	3850	1.047
13052072-7739015	II	4350	1.95
13063053-7734001	II	3560	0.125
13070922-7730304	II	4060	0.89
13072241-7737225	III	3705	0.29
13080628-7755051	II	4350	1.175
13095036-7757240	II	3487	0.33
13100415-7710447	II	3415	0.23

**Notes.**
<sup>a</sup> References: Luhman et al. (2008); Alcalá et al. (2008); Spezzi et al. (2008)

piled photometry for Chamaeleon I and II members.

Cloud	2MASS J	Filter	$\lambda_{eff}$ (Å)	Flux (erg/cm <sup>2</sup> /s/Å)	Flux error (erg/cm <sup>2</sup> /s/Å)
Chal	10463795-7736035	GALEX/GALEX.FUV	1542.3	2.409492947054E-16	1.3892712556971E-17
Chal	10463795-7736035	GALEX/GALEX.NUV	2274.4	7.1026990635684E-15	3.8503326252756E-17
Chal	10463795-7736035	TYCHO/TYCHO.B	4280.0	5.7787397363199E-13	1.4370523170994E-14
Chal	10463795-7736035	TYCHO/TYCHO.V	5340.0	6.7712367865798E-13	1.2473079108729E-14
Chal	10463795-7736035	DENIS/DENIS.I	7862.1	2.8492382854225E-13	2.0993963527685E-14
Chal	10463795-7736035	2MASS/2MASS.J	12350.0	2.2793213744817E-13	3.7787986216975E-15
Chal	10463795-7736035	2MASS/2MASS.H	16620.0	9.8226780523406E-14	4.9758614524518E-15
Chal	10463795-7736035	2MASS/2MASS.Ks	21590.0	4.3746979677725E-14	9.2672651807888E-16
Chal	10463795-7736035	WISE/WISE.W1	33156.6	8.674311371174E-15	2.1571207259674E-16
Chal	10463795-7736035	WISE/WISE.W2	45645.0	2.5436716474833E-15	4.6856163335733E-17
Chal	10463795-7736035	AKARI/IRC.S9W	82283.6	3.304074731026E-16	3.9850807530467E-17
Chal	10463795-7736035	WISE/WISE.W3	107868.4	6.8415691439533E-17	1.0082108879075E-18
Chal	10463795-7736035	WISE/WISE.W4	219149.6	5.4364535147677E-18	4.0557985702824E-19
Chal	10555973-7724399	GALEX/GALEX.FUV	1542.3	3.4666792373282E-17	6.336030288325E-18
Chal	10555973-7724399	GALEX/GALEX.NUV	2274.4	2.5294576603161E-17	3.2778926195947E-18
...					

## References:

- GALEX: Bianchi & GALEX Team (2000)  
 Johnson: Mermilliod & Mermilliod (1994)  
 Tycho-2: Høg et al. (2000)  
 Stromgren: Hauck & Mermilliod (1998)  
 WFI: López Martí et al. (2004); Spezzi et al. (2007)  
 DENIS: DENIS Consortium (2005)  
 2MASS: Skrutskie et al. (2006)  
 WISE: Wright et al. (2010)  
 Spitzer: Alcalá et al. (2008); Luhman & Muench (2008b)  
 AKARI: Ishihara et al. (2010)  
 IRAS: Helou & Walker (1988)